The Pennsylvania State University

The Graduate School

Department of Geosciences

MODELING GLACIER-ROCK-CLIMATE INTERACTIONS: MORAINE DEPOSITION, STAGNATION EVENTS, AND SUPRAGLACIAL DEBRIS

A Dissertation in

Geosciences

By

David A. Vacco

Submitted in Partial Fulfillment
of the Requirements
for the Degree of

Doctor of Philosophy

May 2009

The dissertation of David A. Vacco was reviewed and approved* by the following

Richard B. Alley
Evan Pugh Professor of Geosciences
Dissertation Advisor
Chair of Committee

Sridhar Anandakrishnan
Associate Professor of Geosciences

Rudy Slingerland
Professor of Geosciences

David Pollard
Senior Scientist
Earth and Environmental Systems Institute

Derek Elsworth
Professor of Energy and Mineral Engineering

Katherine Freeman
Associate Head of Department of Geosciences
Professor of Geosciences

*Signatures are on file in the Graduate School

ABSTRACT

New, quantitative information on past climates can be extracted from observations of glacial deposits through joint interpretation using a new glacier-flow model that simulates debris transport and deposition. Locations of moraine sets in some northern-hemisphere locations including Greenland and North America are consistent with the hypothesis that temperature anomalies associated with millennial cold events occurred primarily in wintertime. Extensive forward simulations show that glacier stagnation is more likely for larger and faster warming, suggesting that glacial deposits can be used to learn the amplitude of abrupt-warming events. Additional data will be required on supraglacial-debris effects before such temperature-change reconstructions are quantitatively accurate for heavily debris-laden glaciers, but existing understanding is sufficient to show that well-defined moraine ridges lacking extensive, homogeneous, hummocky deposits just upglacier represent climatically significant events and not landslide-triggered advances.

The first chapter of this work involves the coupling of a dynamic glacier model with a dynamic subglacial sediment package, allowing sediment to be deposited sub- and pro-glacially. The result is a numerical glacier model that deposits moraines based on its terminus position. Experiments were run, varying the climate forcing on the glacier, to observe the resulting moraines and compare them to moraine sets observed in nature. Successful simulation of moraine sets in Greenland driven by ice-core climate records required notable damping of the millennial signal, as required by the hypothesis that millennial temperature fluctuations occurred primarily in wintertime.

The second chapter involves testing of the hypothesis that, if the influence of valley hypsometry is controlled for, stagnation of terminal regions of a glacier require warming larger and faster than some threshold, although with some tradeoff between rate and size of warming. Quantitative modeling experiments were run using simplified valley shapes, in order to isolate a cause and effect relationship between hypsometry, climate change, and glacial stagnation. Stagnation was found to be more likely for rougher beds with lower mean slopes, as well as for larger and faster warmings. The results indicate that it may be possible to quantify ancient climate changes based on observations of glacial stagnation deposits.

The third chapter expands on the study of glacier stagnation, to include transport of supraglacial debris and its thermal shielding effects on glacial melting. Modern observations and process understanding show that extensive supraglacial debris favors stagnation. The ice-flow model from the first two chapters was expanded to include “point” sources (landslides) and distributed sources of supraglacial debris, transport of the debris, and the thermal effects of the debris. The results show that landslide deposits sufficient to cause notable glacier advance cause stagnation events while remaining widely distributed on the glacier surface, thus producing hummocky topography upglacier of any moraine, such that a single moraine ridge formed without such hummocky deposits represents a climatic event rather than a landslide. Model runs show that if sufficient supraglacial debris is supplied from distributed sources, the glacier will be longer and more-likely to experience stagnation following warming than an equivalent clean glacier. A rich range of behavior is simulated, with sensitivity to some parameters that are not yet well-constrained by field glaciology. Quantitative estimation of the size and rate of warming responsible for the observed pattern of stagnation deposits, or lack thereof, in glaciated valleys in a region remains a realistic possibility, but will require improved understanding of debris dynamics.

TABLE OF CONTENTS

LIST OF FIGURES

PREFACE

The three chapters of this dissertation are quantitative studies of glacier-climate interactions, already published or to be published in the scientific literature. My modeling experiments are all designed such that the output represents sediments, or sediment locations, that can be compared to observations of natural glacial valleys. The effort of my doctoral research has been to link numerical modeling and field observations, specifically by using controlled numerical experiments to help interpret field data. The results of my dissertation are that we can use field measurements to make quantitative interpretations about climate history, as constrained by my modeling experiments. The ultimate goal, still far in the future, is a valley glacier model containing a complete description of glacial sediment dynamics, such that the model can be used to informally invert observed glacial deposits for the climate forcing that created them.

Chapter 1, the modeling of moraine deposition, is published in the tribute to G.S. Boulton special issue of Quaternary Science Reviews. Committee member David Pollard had previously developed an ice sheet model that included dynamic subglacial sediment transport and deposition. For the study of Chapter 1, I modified Dave's model to represent valley glaciers, and added processes that allowed the glacier model to deposit moraines. The purpose of this study was to experiment on how varying climate forcings lead to different moraine patterns.

I, David Vacco, am the first author of the QSR paper of Chapter 1. My work was to develop the glacier model, including developing a novel, quantitative law for moraine deposition, run the experiments, and author the manuscript for publication. Richard Alley, second author of the manuscript, contributed the main hypothesis tested by the paper, ideas and guidance for my research, and intensive help with editing the manuscript for publication. David Pollard, third author of the manuscript, contributed his formulation of a glacier model based on the shallow ice approximation glacier model with a coupled ability to simulate subglacial-sediment, helped me with debugging my code, provided intensive help and mentoring through my numerical modeling experiments, and contributed edits and comments to the manuscript for publication.

Chapter 2 involved quantification of the dependence of glacial stagnation on the bumpiness of the subglacial bed. The experiments found that the observed length of stagnation (along glacial flow) is correlated to the magnitude and rate of warming that triggered glacial retreat. This study concluded that we might be able to use observations of glacial stagnation deposits to determine the magnitude and rate of the corresponding climate change.

I am the first author of the manuscript for Chapter 2, which has been submitted and accepted for publication by Quaternary Research, pending editorial approval of revisions. I authored the numerical model code, ran the experiments, and wrote the manuscript. Richard Alley, second author of the manuscript, contributed guidance with the hypothesis testing, conception of the experiments, and intensive help with authoring the manuscript. David Pollard, third author, contributed his formulation for the shallow ice approximation model, and much guidance to me with quantitative hypothesis testing.

Chapter 3 was the study of how supraglacial debris affects glacial stagnation. Surprisingly, we have found no previous modeling experiments assessing the ice-dynamical effects of the insulating influence of supraglacial debris on glaciers. The quantitative relationship between debris cover and melt reduction is well known, however. For this study, I implemented a new treatment of supgraglacial debris and coupled it to my shallow-ice glacier model. The experiments indicated that debris cover plays a very strong role in glacial stagnation.

I am first author of the work of Chapter 3, including the manuscript to be submitted for publication. I authored the model involving dynamic ice and supraglacial sediment, the coupling, and numerical modeling experiments. Richard Alley, second author of the manuscript, provided me with guidance through my hypothesis testing, and significant help with authoring of the paper. David Pollard, third author, provided me with guidance toward authoring of the model and debugging help, and comments and edits of the manuscript for publication.

ACKNOWLEDGEMENTS

Thanks to Richard Alley for mentoring, advising, ideas, and guiding my scientific development. Thanks to Dave Pollard for teaching my how to model glacier dynamics, and frequent help with debugging. Thank you to my doctoral committee, including Richard Alley, Dave Pollard, Sridhar Anandakrishnan, Rudy Slingerland, and Derek Elsworth, for comments and questions that improved this dissertation. Thanks to Patrick Applegate, Byron Parizek, Todd Dupont, and many others for discussions that helped me along. Thanks to my Parents and brother for hanging in with me over a 13-year career as a student. Thanks to my friends for being there.

CHAPTER 1. MODELING DEPENDENCE OF MORAINE DEPOSITION ON CLIMATE HISTORY: THE EFFECT OF SEASONALITY

David A. Vacco, *corresponding author*, dvacco@geosc.psu.edu
Richard B. Alley
David Pollard

Published in *Quaternary Science Review*:
Received 26 September 2007;
Accepted 4 April 2008.
Available online 12 November 2008.

David A. Vacco, Richard B. Alley, and David Pollard, in press, Modeling dependence of moraine deposition on climate history: the effect of seasonality. Quaternary Science Reviews (2008), doi:10.1016/j.quascirev.2008.04.018

1.0 Abstract

A simple shallow-ice flowline glacier model coupled to a model of sediment transport and deposition is used to simulate formation and preservation of moraines. The number, positions, and volumes of moraines formed all are sensitive to the climate history assumed. We drive the model with the GISP2 central-Greenland temperature record, and with reduced-millennial-amplitude versions of that record, to test the hypothesis that the Younger Dryas and other millennial oscillations were primarily wintertime events and thus had less influence on glacier behavior than did the Last Glacial Maximum with its strong summertime as well as wintertime signal. We find that the reduced-amplitude Younger Dryas provides a better match to observed moraines.

1.1 Introduction

Glaciers are sensitive to climate (e.g., Oerlemans, 1994). Although ice-dynamical events such as surges (e.g., Kamb et al., 1985) do occur, averaging over several surge cycles or over several glaciers should remove non-climatic effects. Then, glacier extent is primarily controlled by climate.

In the simplest interpretation, glacier fluctuations are driven primarily by changes in summertime temperatures (e.g., Oerlemans, 2001; Denton et al., 2005). For an initially steady glacier on which snow accumulation is balanced by melting, a 1^{o}C temperature rise increases meltwater loss about 35% but increases saturation vapor pressure (hence precipitation, all else being equal) by only about 7%.

However, glaciers undoubtedly are influenced by numerous climatic factors, and fluctuations in glaciers can result from changing snow accumulation or other forcings, especially if temperature does not change at the same time. Thus, using glacier-length records solely as summer-temperature records will at least occasionally lead to errors. We thus wish to be able to test hypotheses for changes in glaciers, and to conduct formal inversions to learn what forcings are consistent with an observed glacier-length change. Although historical changes in glaciers are of great interest, proxy evidence is all we have available for most time periods, with ages of moraines especially important. These ice-marginal deposits are classically interpreted to represent near still-stands of the glacier margin, either during retreat or when advance switched to retreat, allowing sediment deposits to build up at the toe of a glacier (Sugden and John, 1976). The sediment that composes glacial moraines is transported to the toe by various processes, including subglacial water transport, subglacial till deformation, glacial bulldozing of pro-glacial sediments, and melt-out of material carried in or on the ice, with subglacial stream transport and till deformation especially important (e.g., Boulton and Jones, 1979; Boulton and Hindmarsh, 1987; Hart and Boulton, 1991; Alley et al., 1997).

Because of lags in ice-flow, sediment transport, etc., times of moraine formation and volumes of sediment deposited are not simple functions of climate (e.g., Oerlemans, 2001). Thus, complete testing of hypotheses regarding climatic change in glaciated regions can be improved by driving a moraine-depositing glacier model with the suggested climate history, and comparing modeled and observed moraines. Furthermore, if the model is computationally efficient, inversions or other optimizations can be conducted to help generate hypotheses.

To this end, we have coupled a numerical glacier model based on the shallow-ice approximation to a subglacial-sediment transport model. We have incorporated the ability to vary the relative importance of different sediment-transport mechanisms. The climate forcing, glacial domain length, elevation, and shape can all be prescribed within the ranges observed in nature, giving this model the flexibility to simulate important aspects of a great range of natural glacial settings, from large ice sheets to small alpine glaciers.

Here we describe the model, and then use it to address the Denton et al. (2005) hypothesis of changing seasonality associated with the Younger Dryas event. Denton et al. (2005) noted that in the well-calibrated central-Greenland ice-core records, during the Younger Dryas mean annual temperatures cooled most of the way to last glacial maximum (LGM) values after a long warming trend. However, in many moraine records and other climate records especially from Greenland and northwestern Europe, the Younger Dryas was much warmer than the LGM and not much colder than the Little Ice Age; in these locations, the Younger Dryas moraines are located not nearly as far downstream as LGM moraines, but are closer to the Little Ice Age moraines. Denton et al. (2005) suggested that this disparity is best explained by extreme wintertime cold during the Younger Dryas, with summers then only slightly reduced in temperature, in comparison to cold temperatures year-round during the LGM.

We show here that this hypothesis has implications not only for the relative positions of moraines, but also for numbers and volumes of late-glacial moraines. We have not yet attempted detailed hypothesis-testing for a single moraine set (which will require better calibration of the model to local conditions), but we find robust results from the model that, when compared to available data, support the Denton et al. (2005) hypothesis. We note that use of information from suites of moraines partially offsets difficulties introduced by dating errors, which may be as large as the duration of a climate event of interest (e.g., Gosse et al., 1995, Ivy-Ochs et al., 1999, Licciardi et al., 2004, Rinterknecht et al., 2004, Benson et al., 2005, Schaefer et al., 2006).

1.2 Model Description

1.2.1 Ice Model

The dynamic glacier model used for this study implements the shallow-ice approximation in one dimension (Hutter, 1983), following the approach of Schoof (2002, Chapter 2). The shallow-ice model is appropriate for a glacier if it satisfies the condition of small aspect ratio, ε:

$$\varepsilon^2 << 1 \tag{1.1}$$

where ε = [D]/ [L], with [D] the ice thickness scale, and [L] the ice length scale. If we apply scales typical of valley glaciers, [L] = O(10 km). The valley-glacier thickness scale can be calculated as [D] = O(300 m), from assumed steady-state with snowfall rate of O(1 m/yr) and Glen's power-law creep with strain rate proportional to stress raised to the power n=3 [Paterson, 1994]. Then $\varepsilon^2 \sim 0.02 << 1$. This aspect ratio is sufficiently small that the shallow ice approximation is adequate for our purposes (Schoof, 2002). Applying the shallow ice scaling to the stress tensor yields the planar stress-strain relation where vertical shear is the only important stress to ice flow,

$$\tau_{xz} = \rho g (s - z) \frac{dH}{dx} = A^{\frac{1}{n}-1} \left| \frac{\partial u}{\partial z} \right|^{\frac{1}{n}-1} \frac{\partial u}{\partial z}, \tag{1.2}$$

where x is the horizontal axis (perpendicular to gravity), z is the vertical axis, τ_{xz} is the vertical shear stress, s is the ice surface elevation, A is the ice stiffness, taken as 6×10^{-24} Pa^{-3} s^{-1} for temperate ice, H is the ice thickness, and u is the horizontal ice velocity. The mass conservation equation for ice gives us mass transfer over time,

$$\frac{\partial D}{\partial t} + \frac{\partial Q}{\partial x} = b(x,t), \tag{1.3A}$$

where D is glacier surface elevation, Q is the vertically integrated mass flux, and b(x,t) is the surface mass budget = snowfall rate – melt rate, in units of length/time (e.g., meters/yr). Once we apply the scaling argument that [D] << [L], we solve equation (1.2) for du/dz, vertically integrate twice to obtain the ice flux, and insert the result into equation 1.3A to obtain:

$$\frac{\partial D}{\partial t} = \frac{\partial}{\partial x} \left[A' H^{n+2} \left| \frac{\partial D}{\partial x} \right|^{n-1} \frac{\partial D}{\partial x} \right] + b(x,t), \tag{1.3B}$$

where $A' = A(\rho g)^n$.

1.2.2 Sediment Model

To this fairly standard ice-flow model, we couple a dynamic sediment-deformation model following the work of Clark and Pollard (1998), and ice-sediment coupling of Pollard and DeConto (2005). In regions of the domain where subglacial sediment is present, it deforms as a weakly non-linear dynamic sediment layer (Boulton and Hindmarsh, 1987), following the till measurements of Jenson et al. (1995, 1996).

Our use of a weakly nonlinear relation may require additional comment. Under sufficiently high stress, applied for sufficiently long time, there is little doubt that till exhibits nearly plastic or frictional behavior (e.g., Iverson et al., 1998; Rathbun et al., in review). However, owing to dilation and perhaps other processes, strains of order 1 or less at stress below the ultimate strength of the material likely yield low-stress-exponent flow laws (Jenson et al., 1996; Rathbun et al., in review). Because of strong non-steadiness in the subglacial environment, the till may never experience strains in excess of order one under sufficiently steady conditions to reach the frictional/plastic behavior (Iverson et al., 1998; Alley, 2000).

With these considerations, the stress-strain relation is written as

$$\tau = c + p'\tan\phi + \left(\frac{1}{D_0}\right)^{\frac{1-m}{m}} \mu_0 \left(\frac{du_{sed}}{dz}\right)^{\frac{1}{m}}, \qquad (1.4)$$

where c is the sediment cohesion, p' is effective pressure (overburden pressure minus pore-water pressure), ϕ is the sediment angle of internal friction, D_0 is the reference deformation rate, μ_0 is the viscosity, u_{sed} is the horizontal sediment velocity, and m is the power law exponent, where m ~ 1.5 gives a weakly non-linear sediment. We use equation (1.4) to calculate the subglacial sediment flux via deformation, where τ is a boundary condition imparted on the bed from the ice above, and the sediment velocity at the ice-sediment interface is imparted to the ice flux in equation 1.3B. Equation 1.4 is solved for du/dz, and integrated vertically to obtain the mass flux. We use the result to solve for the dynamic sediment-mass continuity equation:

$$\frac{dh_{sed}}{dt} = -\frac{\partial}{\partial x}\left[\int_{z_d}^{0} u_{sed}\,dz\right] + Q_{quarry} - \frac{\partial}{\partial x}\left(Q_{sedwater}\right) \qquad (1.5)$$

where u_{sed} is the basal ice velocity due to sediment deformation, h_{sed} is the sediment thickness, z_d is the depth where sediment velocity is zero, Q_{quarry} is the flux of sediment into the domain by glacier bed erosion (explained below), and $Q_{sedwater}$ is the flux of sediment transported by subglacial water (explained below). The resulting system of equations (1.3) – (1.5) is a coupled dynamic ice- and sediment-transport model that can be solved numerically.

1.2.3 Sediment Source

Sediment enters into the domain via glacial erosion of the bed. Erosion rate is taken to be linearly proportional to the work done by the glacier on the bed,

$$Q_{quarry} = A_{quarry} u_{bed} \tau_{bed}, \qquad (1.6)$$

where Q_{quarry} is the quarrying rate in meters/yr, u_{bed} is the glacial sliding velocity, τ_{bed} is the shear stress exerted on the bed, and A_{quarry} is the quarrying coefficient. A_{quarry} is a parameter that was tuned to match observed quarrying, which often is on the order of mm/yr (Hallet et al., 1996).

1.2.4 Subglacial Sediment Transport by Water

Although other mechanisms can be specified, sediment transport initially is modeled for deforming till and in water beneath the glacier. For transport in subglacial streams, we follow Alley et al. (1997), such that,

$$Q_{sedwater} = A_{water} Q_{water}^{3}, \qquad (1.7)$$

where $Q_{sedwater}$ is the mass flux of sediment due to subglacial water, Q_{water} is the flux of subglacial water, and A_{water} is the subglacial fluvial sediment coefficient, which can be calculated from general sediment-transport relations or tuned to a particular situation. Meltwater flux is dominated by surface melt, which we route immediately to the bed, so that Q_{water} is the integrated up-valley surface melt.

1.2.5 Glacial Bulldozing

In addition to the sediment transport mechanisms described above, we include sediment transport at the glacier toe by bulldozing. At every time-step in the model, we test for advance of the glacier terminus. In any time-step that the terminus advances, we instantaneously transport all sediment to the toe that was overrun by the recent advance. This mechanism allows advancing ice to "bulldoze" its moraines. In reality, this need not be an instantaneous process, but it can be spectacularly fast (Nolan et al., 1995).

1.2.6 Sediment Sink

Glaciofluvial sediment transport is highly efficient in many or most glacial environments, removing most of the sediment from the system so that moraines represent only a small subset of the total glacial transport (e.g., Bell and Laine, 1985; Alley et al., 1997). Our modeling experiments show that, for geomorphically active glaciers, important ice-dynamical effects would be produced rapidly by sedimentation if all of the sediment were retained beneath or just in front of the glacier. For the model runs reported here, we introduced a sediment sink to account for the loss in proglacial streams. We specify instantaneous loss of 80% by volume of the sediment reaching the ice front. We obtain relatively large moraines, and even higher losses probably are appropriate for some glacial settings.

1.3 The Climate Forcing

Denton et al. (2005) reviewed and extended evidence indicating that millennial-scale climate changes around the north Atlantic during the last ice age should be interpreted differently from the slower orbital-scale changes. In particular, Denton et al. (2005) argued that the millennial-scale oscillations primarily reflected changes in north Atlantic sea ice linked to oceanic and atmospheric circulation with dominant wintertime impacts (Alley, 2007), whereas the orbital-scale changes from Milankovitch forcing included associated Earth-system response with important greenhouse-gas concentration changes, yielding strong changes in summertime as well as wintertime.

We thus separate millennial from orbital climate changes for use in our initial experiments, using a digital filter with a 10,000-year-frequency cutoff (Figure 1.1B). (We do not focus here on sub-millennial changes, such as result from El Nino, NAO, volcanic eruptions, etc., choosing to discard this high-frequency information for our initial experiments, Figure 1.1A.) The time schedule of climate changes is taken from the oxygen-isotopic history of the GISP2 ice core, central Greenland (Stuiver and Grootes, 2000). We reconstruct a temperature history with millennial and orbital amplitudes scaled independently. We specify sea-level temperature to give a selected amplitude between LGM and modern in the orbital band. We then add the millennial variations, scaled by an additional factor $0 \leq \alpha \leq 1$.

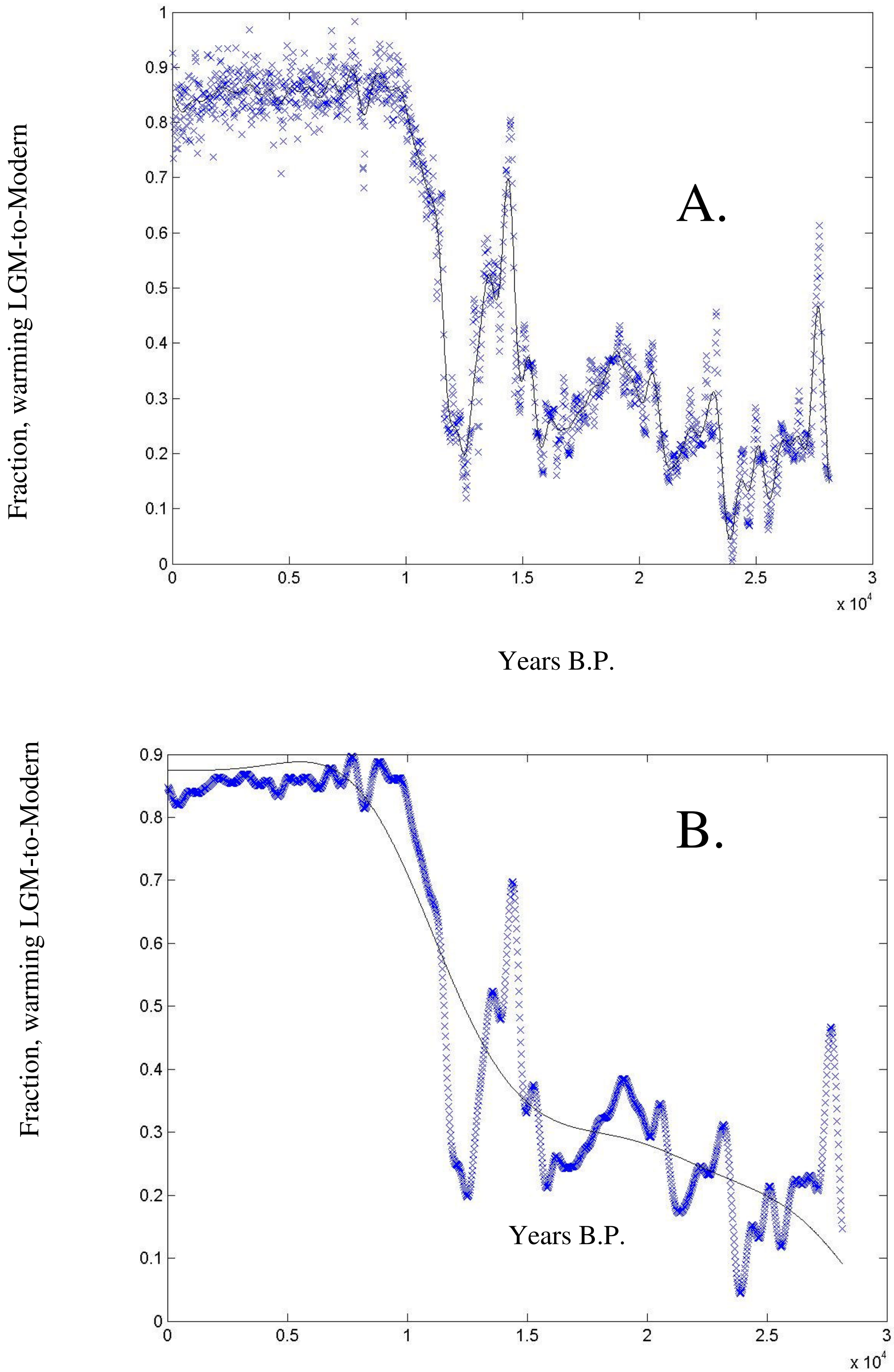

Figure 1.1. The GISP2 time series through the last deglaciation (Stuiver and Grootes, 2000, blue Dashed line, 1.1A), and smoothed with a 800 yr low pass filter (thick black line, 1.1A). The time-series was seperated into a deglacial signal (1.1B., blue line) using a 10,000 yr low pass filter, and the full signal including the millennial scale variability (1.1B, black line).

As discussed below, this additional scaling is suggested by the Denton et al. (2005) seasonality hypothesis. Once sea-level temperature is determined, the temperature at higher elevations is taken from the assumed lapse rate. Hence

$$\text{Temp}(t,z) = L(t) + \alpha\, YD(t) - \gamma z, \qquad (1.8)$$

where t = time in kyr, z = meters above sea-level, L(t) is the deglaciation time series, YD(t) is the millennial time series, γ is the temperature lapse rate with elevation = 0.008 $^{o}C\ m^{-1}$, and the strength of the millennial scale signal is controlled by a fraction $0 \leq \alpha \leq 1$. Decomposing the temperature record like this allows us to test the effect of weakening the millennial scale signal in GISP2 (termed "weakening the Younger Dryas" for convenience, where, for example, "Younger Dryas = 10 %" means $\alpha = 0.1$).
To calculate mass balance of the model glacier in a simple way from this time-series of millennial and orbital changes, the temperature cycle over a single year is assumed to be sinusoidal about the mean annual temperature with an amplitude of 13 ^{o}C. This assumption allows the annual amount of melt at the ice surface to be calculated using the positive degree-day parameterization (Van der Veen, 1999).

For simplicity, the ice-equivalent snowfall rate was assumed to be 1.0 m/yr at sea-level. The modeled snowfall rate was allowed to vary with temperature as a function of saturation vapor pressure, where the snowfall rate was modeled to increase 7 % per ^{o}C of mean annual temperature increase. Clearly, hypotheses for mass-balance changes driven by dynamical changes in the atmosphere rather than by thermodynamic effects on saturation vapor pressure can be tested in this framework, but are beyond the current contribution.

1.4 Results and Discussion

The model output is a plot of glacial till strata labeled by age of deposition (figure 1.2 – 1.3). The results show morphologic and stratigraphic relationships between the tills deposited by the GISP2-driven glacier model. The resulting moraines are correlated with advances in the modeled glacier caused by cold events in the GISP2 deglaciation record. When the temperature forcing includes the millennial-scale signal at full strength, and a 15^{o}C warming between typical glacial and interglacial conditions (Cuffey et al., 1995), the resulting moraines (figure 1.2A) correspond to the two cold events (24 kyr and 21 kyr) during the time often identified as the LGM, plus the Younger Dryas cold event (12.8 – 11.5 kyr). The Younger Dryas moraine is partially cored by sediments deposited during the pre-Bϕlling or Heinrich Event 1 (H1) cold event, ~ 16 kyr. In this case the "Younger Dryas moraine" contains sediments that are older than the Younger Dryas cold event in GISP2. Cosmogenic dates on a moraine with a similar complicated sedimentary structure

0.8

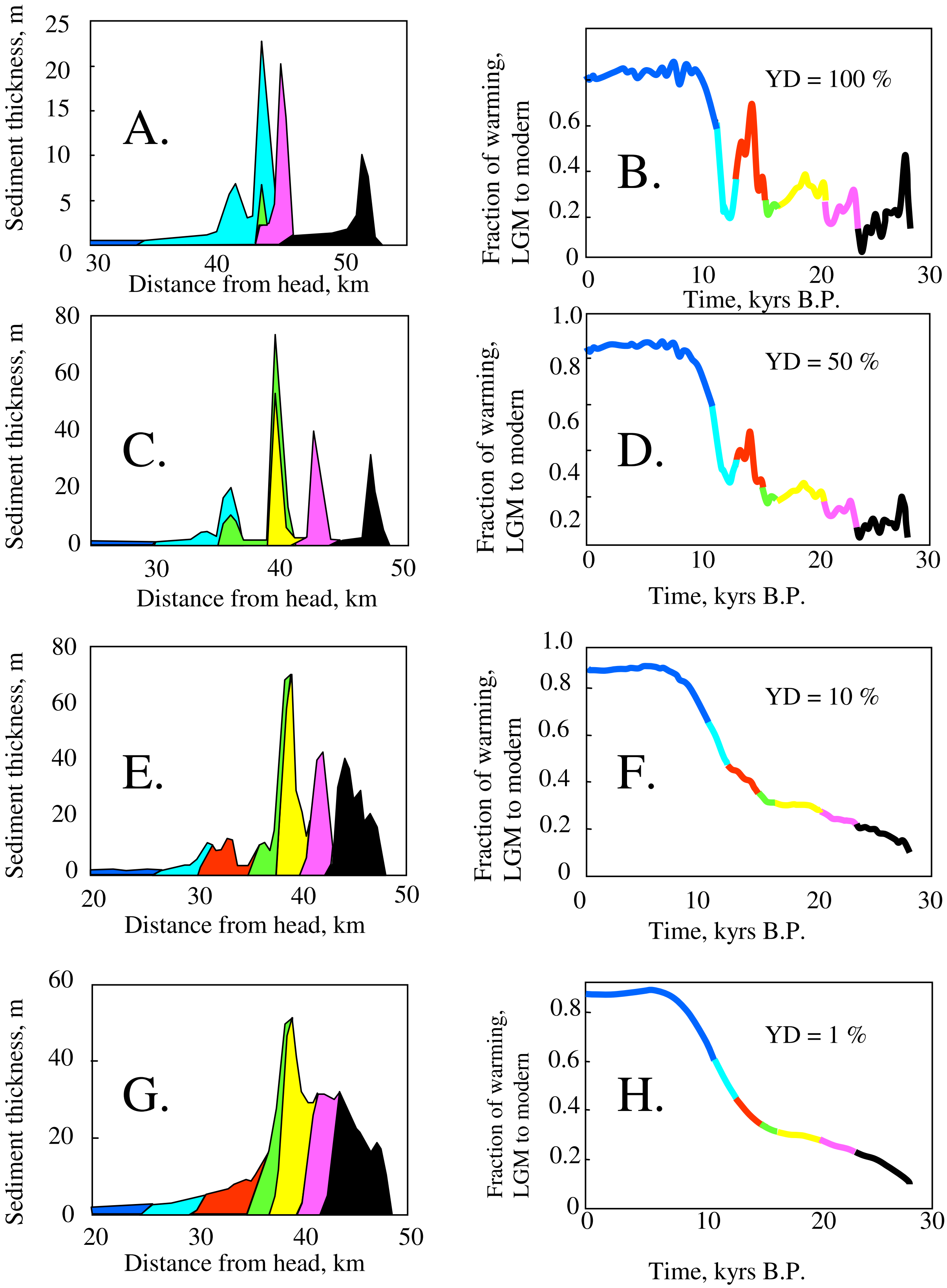

Figure 1.2. Modeled sediment distribution from the coupled ice-sediment model, driven by GISP2 with warming = 15 ^{o}C from LGM to modern, with millennial scale signals at 100% (A-B), and reduced millennial scale variability to 50% (C-D), 10% (E-F), and 1% (G-H). The sediments are color coded by time period:

23.5 kyr, 21 kyr, 16.5 kyr, 15.5 kyr, 13 kyr, 11.6 kyr, Holocene.

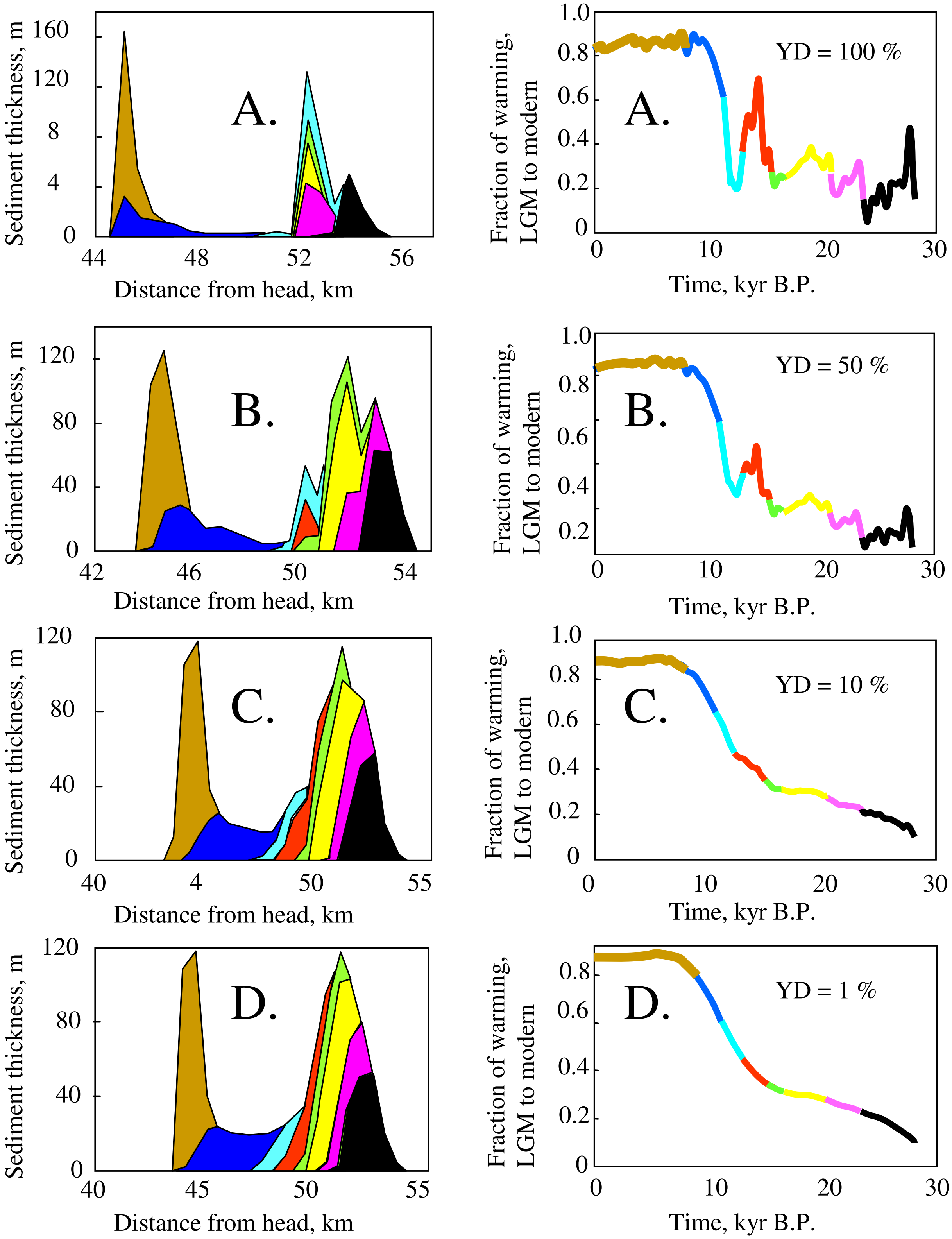

Figure 1.3. Modeled sediment distribution from the coupled ice-sediment model, driven by GISP2 with warming = 3 °C from LGM to modern, with millennial scale signals at 100% (A), and reduced Millennial scale variability to 50% (B), 10% (B), and 1% (D). The sediments are color coded by time period:

23.5 kyr, 21 kyr, 16.5 kyr, 15.5 kyr, 13 kyr, 11.6 kyr, 7.8 kyr, Holocene.

could potentially yield both Younger Dryas exposure ages and ages on the order of 15 – 17 kyr, if the older boulders protruded through the younger surface.

The number of moraines deposited is influenced by the relative strengths of orbital and millennial signals. With the full amplitude of the Younger Dryas as indicated by GISP2, moraines younger than about 21 kyr are buried or overrun by the large Younger Dryas re-advance. Reducing the Younger Dryas amplitude allows the orbital warming between LGM and Younger Dryas to become evident, so that the Younger Dryas cooling is no longer strong enough to overrun older but post-LGM moraines (figures 1.2B - D). This allows persistence of the prominent moraine that corresponds to 20 – 15 kyr and especially to the Heinrich Event 1 (H1) cooling. Such a moraine has been observed by cosmogenic exposure aging of moraines in many places (Clark et al., 1995; Gosse et al., 1995; Licciardi et al., 2004; Benson et al., 2005).

With the millennial scale signals in GISP2 dampened to 10% of their observed strength, the inner-most deglacial moraine contains only a thin surface of sediments deposited during the Younger Dryas. Most of this moraine is cored by sediments of Bolling-Allerod age. Such a moraine could yield a wide range of exposure age dates, and many of them would be discordant with the Younger Dryas cold event. If any post-glacial erosion were to occur, it is likely that Younger Dryas sediments would be completely stripped off this moraine. In such a case, the measured exposure age would not fully reflect the deposition history of the moraine. When the millennial scale signals are dampened to 1% of full GISP2 strength (figure 1.2D), the only moraine deposited represents the slowest period (17-15 kyr) of retreat during a steady warming between LGM and modern.

For these runs, the warming was sufficient to remove ice from the model domain as the Holocene began, so we did not simulate Holocene or Little Ice Age deposits. To consider those, we used the same domain but set the amplitude of the glacial-interglacial warming to just 3^{o}C. Sediment deposition then occurs over a smaller spatial distance, decreasing the number of distinct moraines (figure 1.3). Modeling the temperature history with the Younger Dryas signal at 100% (figure 1.3A) yields three moraines, corresponding to the time periods of the LGM, the Younger Dryas, and late-Holocene. The "Younger Dryas" moraine is cored by sediments ranging from LGM to Younger Dryas.

Decreasing the strength of the Younger Dryas signal in this case leads to a change in the number of moraines, from three moraines (figure 1.3A), to four moraines (figures 1.3B), to two moraines (figures 1.3C-D). Weakening the millennial scale signal to 50% causes all of the late glacial sediments to be deposited in the same package, yielding a single deglacial moraine, representing an ~ 5 km region where the glacial terminus slowly retreated during the last deglaciation. Weakening the millennial scale signal to 10 % or 1 % yields two distinct moraines. The outer-most moraine corresponds to the LGM, the inner-most moraine to the modern ice location, and the middle deposits could be tied to the deglaciation. Attributing the deglacial moraine to a specific millennial scale event, in this case, would be difficult, as if contains sediments deposited 20 – 11 kyr. Cosmogenic exposure dates on this moraine would potentially yield dates spanning 10,000 years. (Clearly, adding in the high-frequency (sub-millennial) oscillations, or allowing ice-flow effects, could break up these fairly broad moraines into discrete smaller ridges, and this would be aided by higher spatial resolution in the modeling. Thus, single moraines simulated here might correspond to bands of similar-aged moraines in some settings.)

The Denton hypothesis (Denton et al., 2005) states that the large millennial changes in the GISP2 ice core record were primarily caused by large shifts in winter temperatures, with more-muted changes in summer temperatures for the Younger Dryas and other millennial events. The GISP2 ice core indicates that mean temperatures during the Younger Dryas were not much warmer than during the LGM, and were much colder than during the Little Ice Age. Observations of moraines around Greenland imply the opposite, that Younger Dryas climate conditions were much closer to the Little Ice Age than to the LGM.

In our model, variability in the below-freezing mean winter atmospheric temperature does not affect glacial advance/retreat. To further test the seasonality effects, we separated winter and summer temperature histories, and then varied only the summertime strength of the millennial oscillations. The results were the same as those plotted in figures 1.2-1.3, indicating that winter temperature fluctuations do not affect the modeled terminus position as long as mean winter temperature is below freezing. Thus the applied climate forcing controls the glacier position by the amount of melt taking place in the summer season. It follows that our modeled terminus position is dominantly controlled by variations in the summer-season mean atmospheric temperature.

1.5 Conclusions and future work

The results show that our ice-sediment coupled model can be used to simulate many glacial settings by adjusting the domain, climate forcing, sediment parameters, and sediment transport processes. The coupled ice-sediment model, when driven by GISP2 climate, yields moraines similar to those observed in nature (Clark et al., 1995; Gosse et al., 1995; Ivy-Ochs, 1999; Kelly et al., 2004; Licciardi et al., 2004; Rinterknecht et al., 2004; Benson et al., 2005), but reveals that moraine deposition of the last deglaciation may be more complex than in some interpretations. Processes including reworking of sediments, erosion and bulldozing due to advances, and interaction of glacial sedimentation processes all affect the preserved moraine morphology.

Using our model, we find that the GISP2 climate record generates Younger Dryas moraines that are far downvalley of those from the Little Ice Age and close to LGM positions, but that reducing the amplitude of the millennial oscillations shifts the Younger Dryas moraines upvalley toward those of the Little Ice Age, providing model-based support for the arguments in Denton et al. (2005) that Younger Dryas cooling was strongest in wintertime. We also find that the full GISP2 climate record causes the Younger Dryas glacial advance to remove the Heinrich Event 1 moraine, contrary to observations in many places, again supporting the Denton et al. (2005) seasonality hypothesis.

Using the parameterizations here, the sizes as well as number and position of moraines provide information on the paleo-climatic forcing. Some of the model parameters, such as the fraction of transported sediment preserved in moraines rather than transported away in proglacial streams, may prove to be functions of climate, which would complicate interpretation of moraine sizes. We nonetheless believe that comparison of models and data for moraine sizes, numbers and positions will prove instructive; if climatic history can be constrained by numbers and positions, for example, then the sizes will yield important geomorphic information on the climatic response of glacial sedimentary processes.

1.6 Acknowledgements

We thank Sridhar Anandakrishnan, Meredith Kelly, and Patrick Applegate for discussions that helped improve this study. Partial support was provided by the National Science Foundation through grants 0424589, 0440899, and 0531211, and by the Gary Comer Science and Education Foundation

1.1.7 References

Alley, R. B., 1992. Flow-law hypotheses for ice-sheet modeling. *Journal of Glaciology* 38, no. 129, p. 245-256.

Alley, R. B., Cuffey, K. M., Evenson, E. B., Strasser, J. C., Lawson, D. E., and Larson, G. J., 1997. How glaciers entrain and transport basal sediment: physical constraints. *Quaternary Science Reviews* 16, p. 1017-1038.

Bell, M. and Laine, E. P., 1985. Erosion of the Laurentide region of North America by glacial and glaciofluvial processes. *Quaternary Research* 23, p. 154-174.

Benson, L., Madole, R., Landis, G., and Gosse, J., 2005. New data for Late Pleistocene Pinedale alpine glaciation from southwestern Colorado. *Quaternary Science Reviews* 24, p. 49-65.

Boulton, G. S. and Hindmarsh, R. C. A., 1987. Sediment deformation beneath glaciers: rheology and geological consequences. *Journal of Geophysical Research* 92, 9059-9082.

Boulton, G. S. and Jones, A. S., 1979. Stability of temperate ice caps and ice sheets resting on beds of deformable sediment. *Journal of Glaciology* 24, 29-42.

Clark, P. U., and Pollard, D., 1998. Origin of the middle Pleistocene transition by ice sheet erosion of regolith. *Paleoceanography* 13, no. 1, p. 1-9.

Cuffey, K. M., Clow, G, D, Alley, R. B., Stuiver, M., Waddington, E. D., Saltus. R. W., 1995. Large Arctic temperature change at the glacial-Holocene transition. *Science* 270, 455-458.

Denton, G. H., and Karlen, W., 1973. Holocene climatic variations-their pattern and possible cause. *Quaternary Research* 3: 155-205.

Denton, G. H., Alley, R. B., Comer, G. C., and Broecker, W. S., 2005. The role of seasonality in abrupt climate change. *Quaternary Science Reviews* 24, p. 1159-1182.
Gosse, J. C., Evenson, E. B., Klein, J., Lawn, B., and Middleton, R., 1995. Precise cosmogenic ^{10}Be measurements in the western North America: Support for a global Younger Dryas cooling event. *Geology* 23, no. 10, p. 877-880.

Hallet, B., Hunter, L. and Bogen, J., 1996. Rates of erosion and sediment evacuation by glaciers: a review of field data and their implications. *Global and Planetary Change* 12, 213- 235.

Hart, J. K., Boulton, G. A., 1991. The interrelation of glaciotectonic and glaciodepositional processes within the glacial environment. *Quaternary Science Reviews* 10, 335-350.

Hutter, K., 1983. *Theoretical Glaciology; material science of ice and the mechanics of glaciers and ice sheets*. Dordrecht, etc., D. Reidel Publishing Co.; Tokyo.

Iverson, N.R., Hooyer, T.S. & Baker, R.W., 1998. Ring-shear studies of till deformation: Coulomb-plastic behavior and distributed strain in glacier beds. *Journal of Glaciology*, 44, 634-642.

Ivy-Ochs, S., Schuchter, C., Kubik, P. W., Denton, G. H., 1999. Moraine exposure dates imply synchronous Younger Dryas glacier advances in the European Alps and in the Southern Alps of New Zealand. *Geografiska Annaler, Series A, Physical Geography* 81, no. 2, p. 313-323.

Jenson, J. W., Clark, P. U., MacAyeal, D. R., Ho, C., and Vela, J. C., 1995. Numerical modeling of advective transport of saturated deforming sediment beneath the Lake Michigan Lobe, Laurentide Ice Sheet. *Geomorphology* 14, p. 157-166.

Jenson, J. W., MacAyeal, D. R., Clark, P. U., Ho, C. L., and Vela, J. C., 1996. Numerical modeling of subglacial sediment deformation: Implications for the behavior of the Lake Michigan Lobe, Laurentide Ice Sheet. *Journal of Geophysical Research* 101, no. B4, p. 8717-8728.

Kamb, B., C.F. Raymond, W.D. Harrison, H. Engelhardt, K.A. Echelmeyer, N. Humphrey, M.M. Brugman and T. Pfeffer., 1985. Glacier surge mechanism—1982-1983 surge of Variegated Glacier, Alaska. *Science* 227, 469-479.

Kelly, M. A., Kubik, P. W., Von Blanckenburg, and F., Schluchter, C., 2004. Surface exposure dating of the Great Aletsch Glacier Egesen moraine system, western Swiss Alps, using the cosmogenic nuclide ^{10}Be. *Journal of Quaternary Science* 19, no. 5, p. 431-441.

Licciardi, J. M., Clark, P. U., Brook, E. J., Elmore, D., and Sharma, P., 2004. Variable responses of western U.S. glaciers during the last deglaciation. *Geology* 32, no. 1, p. 81-84.

Nolan, M.,Motyka, R. J., Echelmeyer, K.& Trabant,D. C., 1995. Ice-thickness measurements of Taku Glacier, Alaska, USA, and their relevance to its recent behavior. *Journal of Glaciology* 41, p. 541–553

Oerlemans, J., 1994. Quantifying global warming from the retreat of glaciers. *Science* 264, 243–245.

Paterson, W. S. B., 1994. *The physics of glaciers*. Third edition, Pergamon, Oxford.

Pollard, D., and DeConto, R. M., 2003. Antarctic ice and sediment flux in the Oligocene simulated by a climate-ice sheet-sediment model. *Palaeogeography, Palaeoclimatology, Palaeoecology* 198, p. 53-67.

Pollard, D., and DeConto, R. M., 2005. A coupled ice-sheet /ice-shelf / sediment model applied to a marine-margin flowline: Forced and unforced variations. In: *Glacial Sedimentary Processes and Products, International Association of Sedimentologists Special Publication, IAS Conference of Glacial Sedimentary Processes and Products*, edited by Hambrey, M.J., Christoffersen, P., Glasser, N. F., and Hubbard, B., 22-27 August 2005. University of Wales, Aberystwyth, in press.

Rathbun, A.P., C. Marone, R.B. Alley and S. Anandakrishnan. Submitted. Laboratory study of the frictional rheology of sheared glacial till. *Journal of Geophysical Research.*

Rinterknecht V. R., Clark, P. U., Raisbeck, G. M., Yiou, F., Brook, E. J., Tschudi, S., Lunkka, J. P., 2004. Cosmogenic ^{10}Be dating of the Salpausselka I Moraine in southwestern Finland. *Quaternary Science Reviews* 23, p. 2283-2289.

Schaefer, J. M., Denton, G. H., Barrell, D. J. A., Ivy-Ochs, S., Kubik, P. W., Anderson, B. G., Phillips, F. M., Lowell, T. V., Schluchter, C., 2006. Near-synchronous interhemispheric termination of the last glacial maximum in mid-latitudes. *Science* 312, p. 1510-1513.

Schoof, C., 2002. *Mathematical models of glacier sliding and drumlin formation*: Doctoral Dissertation, Corpus Christi College, University of Oxford, 209 p.

Stuiver, M., and Grootes, M., 2000. GISP2 oxygen-isotope ratios. *Quaternary Research* 53, p. 277-284.

Sugden, D. E., and John, B. S., 1976. *Glaciers and Landscapes*. Edward Arnold Ltd., London.

Van der Veen, C. J., 1999. *Fundamentals of Glacier Dynamics*, Balkema, Rotterdam, 462 p.

CHAPTER 2. NUMERICAL MODELING OF VALLEY GLACIER STAGNATION: TOWARD A NEW PALEOCLIMATIC INDICATOR

David A. Vacco, *corresponding author*, dvacco@geosc.psu.edu
Richard B. Alley
David Pollard
David Reusch

Accepted in *Quaternary Research*
Elsevier, 2009

Abstract

Stagnation of the terminal region of a glacier occurs in response to sufficiently large and rapid climatic warming, so the presence of stagnation deposits provides quantitative information on the climate change that forced retreat. Here we use a simple flow-line glacier model to investigate the relationship between stagnation, climate forcing and aspects of the glacier bed. For climatic warming greater than the threshold to cause stagnation, larger or faster warming events cause longer regions of a glacier to stagnate. Smaller or slower warming episodes, below the threshold for stagnation, cause retreat while active flow persists along the entire glacier length. The threshold for stagnation depends not only on the climatic forcing, but also on many other aspects of the glacier, with stagnation favored by factors including a lower mean bed slope with greater roughness. Quantitative determination of the climatic forcing consistent with the occurrence or absence of stagnation deposits requires that these site-specific characteristics be incorporated in modeling.

Introduction

Glacial deposits are important paleoclimatic indicators. Typically, the age of deposition or stabilization of a moraine corresponds to the age of the climate change that forced glacial retreat. However, while the timing of a warming event is obtained by dating moraines, the magnitude or rate of the warming event is not typically obtained. Here we use modeling experiments to suggest that presence or absence of glacial stagnation deposits associated with moraines can be used to place limits on the magnitude and rate of climatic warming events. We review previous work showing that, in response to warming or other climatic change causing negative mass balance, some glaciers stagnate whereas others retreat, that these distinct modes of behavior produce recognizably distinct deposits, and that the topographic setting and climatic forcing together interact to determine the mode of glacial response.

This study isolates the effects of basal topography on glacial stagnation. There are additional factors that play a role in glacial stagnation, such as supraglacial debris (Vacco, 2009, chapter 3). However, investigation of basal topographic control will allow us to understand the stagnation phenomena for “clean” ice, containing no supraglacial debris. Furthermore, investigation of stagnation without debris cover will improve our understanding of stagnation when we consider the effects of both supraglacial debris and basal topography in parallel.

Background

Valley glaciers lose mass by decreasing in length, by thinning, or both. A retreating glacier remains interconnected and flowing along its entire length, as the terminus migrates up-valley. However, thinning can lead to glacial stagnation, where the ice velocity decreases to near zero in a section of a glacier. The non-flowing ice then down wastes until it is gone. Such down-wasting without inflow of ice is especially pronounced if a down-glacier section of the glacier becomes physically separated from the main body.

Stagnation of glacial ice has been observed in modern glaciers, such as Martin River Glacier (Clayton 1964; Tuthill 1966), Muir Glacier (Haselton 1966), Adams Glacier in Glacier Bay (McKenzie 1970), and Burroughs Glacier (Mickelson 1971), all located in Alaska, and in many other glaciers around the world. In many cases the stagnant ice became covered with ablation till, and melted more slowly compared to the clean ice up-glacier. Importantly, Clayton (1964) noted that the surface slope of the stagnant ice was flattening and the ice lobe was thinning, while the glacier length remained constant.

Study of these and other modern stagnation events, combined with process understanding of formation of glacial deposits, has allowed recognition of many more stagnation events for former glaciers, based on characteristics of their sedimentary deposits (e.g., Gravenor and Kupsch, 1959; Mannerfelt, 1961; Clayton 1964; Clebnik and Mulholland, 1979; Paul and Eyles, 1990; Ham and Mickelson, 1994; Johnson et al., 1995; Brown et al., 1998; Eyles et al., 1999; Boone and Eyles, 2001; Braun, 2006). Formation of deposits associated with stagnation requires that ice motion be small enough during deposition that the characteristics of the deposit primarily record depositional processes rather than ice flow processes. This implies a depositional ice motion scale of less than, or perhaps of the same order as, the size of key depositional features such as individual hummocks or basal crevasse fills. Following deposition, ice flow must remain near zero in order to preserve the deposits.

Perhaps the most systematic consideration of stagnation was given by Small (1995). He defined glacial stagnation as a mass wasting event in which a section of glacial ice in the ablation zone ceases flowing, where the stress on the ice was to cause deformation and flow. The onset of stagnation represents a loss of glacial mass in a discrete event, during a dynamic adjustment of glacial mass balance in response to changing climate forcing. As discussed below, Small (1995) argued for a dominant role of topography in controlling stagnation, but suggested the possibility of a climatic influence, which we explore here.

Realistically, stagnation is likely to be realized on a glacier wherever the ice influx rate is small compared to the mass loss by ablation in some section of ice, provided the section under consideration is long compared to the ice thickness at the input; longitudinal stress coupling will maintain flow for shorter segments (Budd, 1968; Kamb and Echelmeyer, 1986). Under such circumstances, the mass balance of that section of the glacier will change primarily in response to ablation rather than ice flow, with motion ceasing as the ice thins by melting.

Under this broad definition, a segment of a glacier might be considered to have stagnated even if the segment remained attached to the active glacier. For this study, we adopt a more restrictive definition. If a segment of a glacier becomes detached from the main glacier, there can be no influx of ice from up-glacier, and stagnation of the mass will follow as the ice thins and the basal shear stress drops to zero. Setting separation as the criterion for stagnation is numerically easy to implement in a computer model.

Conceptual Model

Glaciers in sufficiently close geographic proximity to have experienced similar climatic forcing may nonetheless show a range of stagnation behavior (for example the Knik Glacier and Matanuska Glacier, Alaska; Kopczynski, 2008), consistent with topographic influence on this behavior (Small, 1995). However, as suggested by Clarke (1976), Sharp (1988, p. 122) and Small (1995), whether a glacier stagnates or retreats in response to warming need not be controlled entirely by topography, with the size or rate of warming potentially also important. Figure 2.1A-C shows a cartoon of an initially steady glacier flowing over notable topography. The glacier is subjected to a warming, producing onset or increase in ablation rate below the new equilibrium line but increased accumulation above the new equilibrium line. With the usual sensitivities of ablation and accumulation rate to warming (e.g., Oerlemans, 2001), we expect that the new steady-state glacier will be thicker in the accumulation zone but shorter overall, with thinning in regions close to the new steady terminus. As shown in the figure, a small warming can cause this pattern of response while maintaining a coherently flowing ice mass throughout; the glacier retreats. However, for a large and rapid warming, thinning over the topographic high can isolate the block of ice down-glacier, which must eventually stagnate, producing stagnation deposits. Such an occurrence was observed directly on Burroughs Glacier, Alaska (2.1D, Mickelson, 1971).

The key physical processes controlling stagnation versus retreat in our model can be understood qualitatively. Consider flow of the thin ice over a bedrock obstacle, into the terminal ablation zone of a glacier, as shown with much vertical exaggeration in Figure 2.1. Application of the shallow-ice equations shows that the ice flux increases with the fifth power of the ice thickness. The flow across the bedrock high is balanced by the average melt rate acting over the terminal region, which sets the steady state length. If a small climatic warming causes a small decrease in steady thickness and thus in ice flux over the bedrock high together with an increase in the average melt rate over the terminal region, the glacier must retreat to regain balance, but the continued flow over the bedrock

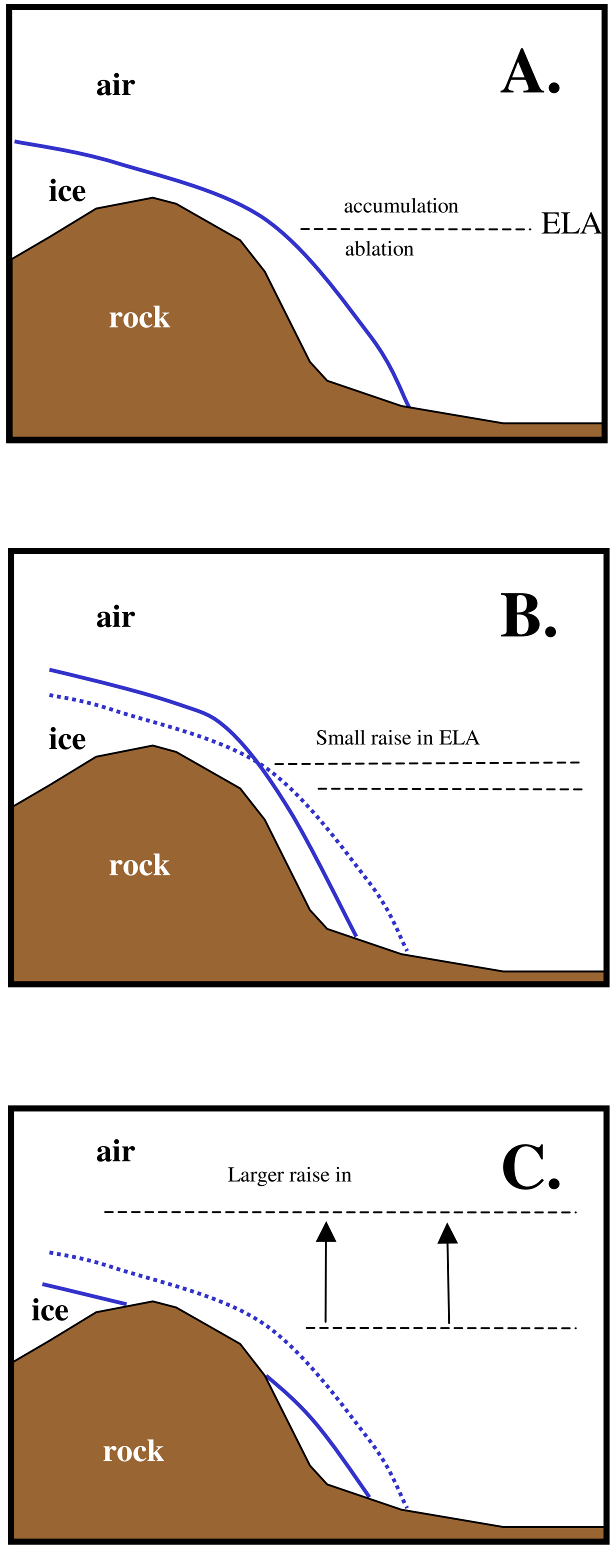

Figure 2.1A-C.

Figure2.1D.

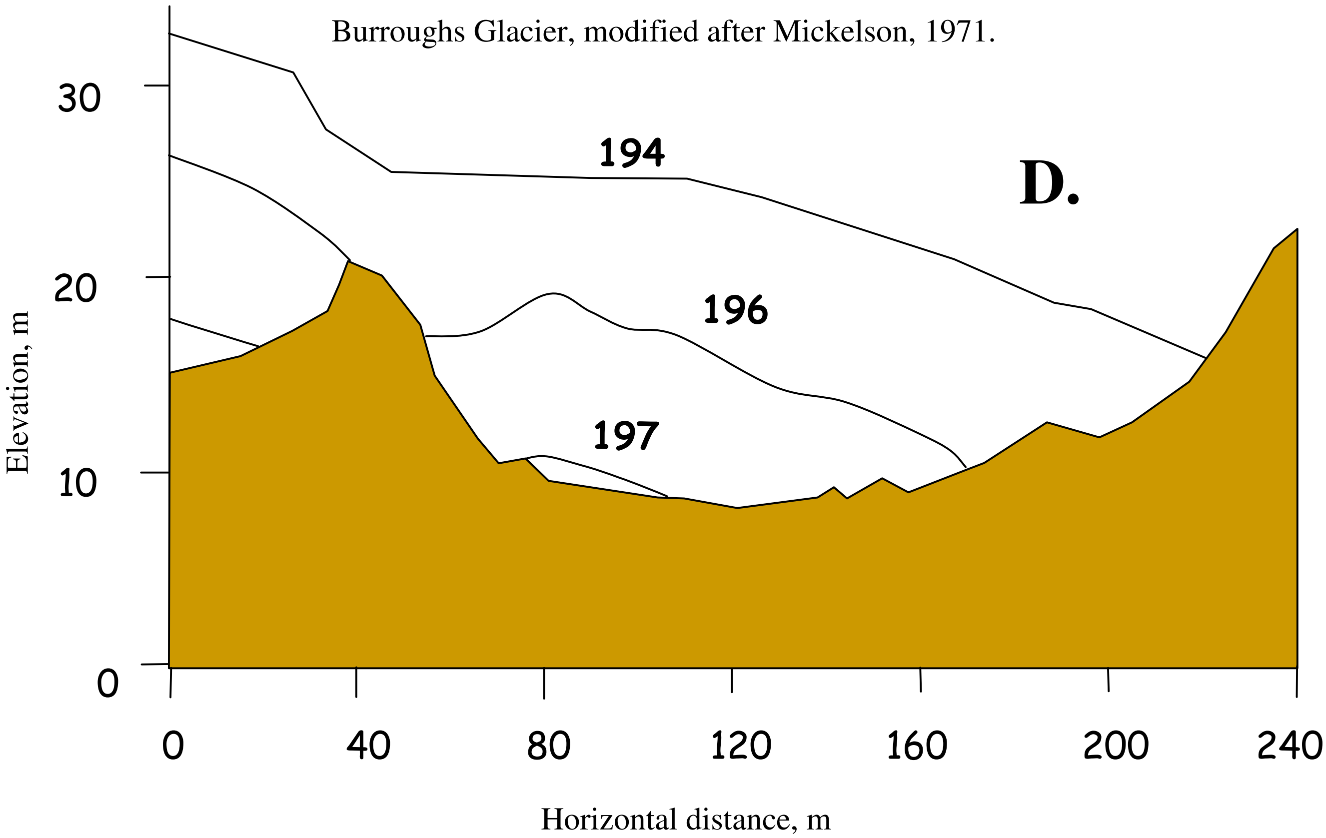

Figure 2.1. (A) Glacier flowing over a bedrock bump, with the ELA marked. (B) Given a small warming (equivalent to a rise in the ELA), the glacier terminus retreats but does not stagnate. (C) Given a Larger warming, melt-down causes the glacier to stagnate. (D) Elevation profiles of Burroughs Glacier, modified after Mickelson, 1971, where the onset of stagnation was observed.

high will allow active flow to continue in the terminal region. A series of such very small perturbations would cause progressive retreat of the terminus, eventually reaching and passing the bedrock high without ever causing stagnation. However, if a sufficiently large climatic warming shifts the ice at the bedrock high well into the ablation zone and triggers notable thinning toward a steady state deglaciation there, the fifth power dependence of ice flux on thickness will greatly reduce ice inflow to the terminal region, causing it essentially to melt downward in place, pinching off first where the ice was initially thinnest over the bedrock high.

We propose that numerical modeling can allow evaluation of the effect of glacial valley topography, in such a way that the existence of stagnation deposits can be used as a quantitative proxy for the climate change. We test the hypothesis that glaciers will be more likely to stagnate if the following conditions are met: (i) the valley contains bumps that protrude into the flowing glacier, creating a section of ice thinner than the surrounding ice; (ii) the toe of the glacier is located down-valley of such a bump before warming; and (iii) the magnitude of warming is sufficient to cause the active toe of the new steady-state glacier to lie up-glacier of the topographic high. If a topographic trough is present, such as an over-deepening, it is likely that a stagnant ice block will reside in the trough down-valley from the bump after a warming event causes retreat.

Model Description

Our model experiments were conducted using a one dimensional shallow-ice model, following Vacco et al., (in press), to simulate ice flow along the central flow-line of a valley glacier. The shallow-ice model simulates the dominant stress in the axes of vertical shear, but not the complete stress state of dynamic ice. We chose the shallow-ice model for its simplicity, numerical stability, and speed of solution, which allowed us to run thousands of experiments exploring parameter space. This model has been established to be an accurate approximation of flow in certain settings (Hutter, 1983; Kamb and Echelmeyer, 1986; Huybrechts et al., 1996; LeMeur et al., 2004). Below, we demonstrate that this model is appropriate for the scale of our experiments. The normal stresses from basal bumps affect local dynamics, so a full-stress-tensor model would provide quantitatively superior results. We prepared a higher-order stress model following Pattyn (2002), and found that: i) for the comparisons conducted, the results were qualitatively and usually quantitatively similar; and ii) the higher-order model was numerically much less stable and much slower to execute. Because we wished to explore much parameter space rapidly, and we were not attempting to quantitatively match behavior in any single glacier, we restricted attention to the shallow-ice model.

Shallow-Ice approximation

All experiments were conducted using the shallow-ice approximation of ice flow (Hutter, 1983), which is obtained by assuming that the only important stress is vertical shear,

$$\tau_{xz} = \rho g H \frac{\partial s}{\partial x}, \tag{2.1}$$

where τ_{xz} is the vertical shear stress, H = ice thickness in meters, ρ = ice density = 920 kg/m^3, g = acceleration due to gravity = 9.81 m/s^2, and $s(x)$ = ice surface elevation in meters as a function of horizontal position x. This assumption allows change in ice thickness to be calculated over time, as a one dimensional shallow-ice thickness evolution equation,

$$\frac{\partial H}{\partial t} = \frac{\partial}{\partial x}\left[A' H^{n+2} \left| \frac{\partial s}{\partial x} \right|^{n-1} \frac{\partial s}{\partial x} \right] + \dot{b}(z,t), \tag{2.2}$$

.

where $\dot{b}(z,t)$ = the local surface mass balance of ice in m/yr, and $A' = A(\rho g)^n$, A = the ice softness parameter = 6.8 x 10^{-15} Pa^{-3} yr^{-1} (Paterson, 1994). The shallow-ice model is appropriate for a glacier if it satisfies the condition of small aspect ratio, ε:

$$\varepsilon^2 << 1 \tag{2.3}$$

where ε = [H]/ [L], with [H] the ice thickness scale, and [L] the ice length scale. We apply the scales of this experiment, [L] = O(10 km), n = 3, and [b] = 1 m/yr (Oerlemans, 2001, chapter 6-8). The valley-glacier thickness scale [H] = O(100 m), assumed steady-state with snowfall rate of O(1 m/yr) and Glen's power-law creep with strain rate proportional to stress raised to the power n = 3 (Paterson, 1994). Then $\varepsilon^2 << 1$, indicating the aspect ratio is sufficiently small that the shallow-ice approximation is appropriate for our purpose of dynamic glacier modeling.

Climate parameterization

Atmospheric temperature was assumed to follow an annual sine wave with a total summer-winter amplitude of 26 ^{o}C. The temperature lapse rate was assumed to be -0.008 ^{o}C m^{-1}. A uniform pre-warming snowfall rate of 1 m yr^{-1} was applied at all elevations. After warming, the snowfall rate was increased by 7% per ^{o}C of warming, reflecting the dependence on saturation vapor pressure. No melting was applied at elevations higher than the equilibrium line altitude (ELA). Below the ELA, the dependence of glacier surface mass balance on atmospheric temperature was parameterized using the positive degree day (PDD) formulation, following van der Veen (1999), with a melting parameter of 0.008 m ^{o}C^{-1} day^{-1}.

Experiment Design

As noted above, for computational simplicity in this study, we define a stagnation event to have occurred when the main part of the glacier is separated from a body of ice toward the terminus ("pinch off"). This narrow definition omits thin ice still connected to the main glacier but with zero or near-zero flow velocity (an assumption that is readily relaxed in future work). Also for simplicity, ice flow in our experiments was limited to the process of internal deformation. We did not allow basal sliding, sediment deformation or other sedimentary processes, or melting at the base of the ice that have been implemented in the model and used in other applications (Vacco et al., 2009). All of these basal processes tend to thin the ice and speed flow; including them would produce thinner ice and easier stagnation, but with similar qualitative dependence on topography and forcing.

We experimented with a wide range of bumpy, one dimensional beds formed as a cosine superimposed on a mean sloping plane (Figure 2.2A), to allow the independent variation of mean slope and bed bumpiness. The total horizontal domain of the model was 200 km, horizontal spacing between computational nodes dx = 250 m, and the time step for forward modeling was dt = 0.1 years. The mean bed slope of the valley was varied from 0.03 to 0.09 at intervals of 0.01, wavelength was varied from 1000 to 7000 m at intervals of 1000 m, amplitude was varied from 10 m to 100 m at intervals of 10 m, and the initial phase of the bed wavesat the ice divide was set to either 0 or π. Note that at wavelength of 1000 m and node spacing = 250 m, there are only 4 computational nodes per wavelength.

The model was initially run to steady state, with an ELA specified so that the glacier terminus remained within the model domain. A warming event was then imposed; in most simulations, the warming was instantaneous. For each set of topographic parameters, seven warming experiments were run, with ELA increase of 100 m to 700 m in steps of 100 m (these are equivalent to mean annual temperature increases of 0.8 to 5.6 ^{o}C). The glacier length, phase relative to bedrock, and locations of any pinched-off ice blocks were recorded until a new steady state was achieved. All combinations of the parameters tested (8 mean bed slopes, 7 wavelengths, 10 amplitudes, 2 phases, and 7 different warming magnitudes) produced a total of 6860 runs.

To supplement this large range of instantaneous-warming simulations, an additional set of experiments was run to assess the dependence of stagnation on rate of warming. The bed parameters for this set of runs were: mean bed slope = 0.03, wavelength = 1000 m, amplitude = 50 m, phase offset = 0 radians, and the total warming = 400 m of ELA increase. Each experiment used a single rate of warming, with rates ranging from 3.0 to 8.0 m/yr of ELA rise, equivalent to warming rates of 2.4 to 6.4 ^{o}C per 100 years assuming an elevation lapse rate of -0.008 ^{o}C m^{-1} .

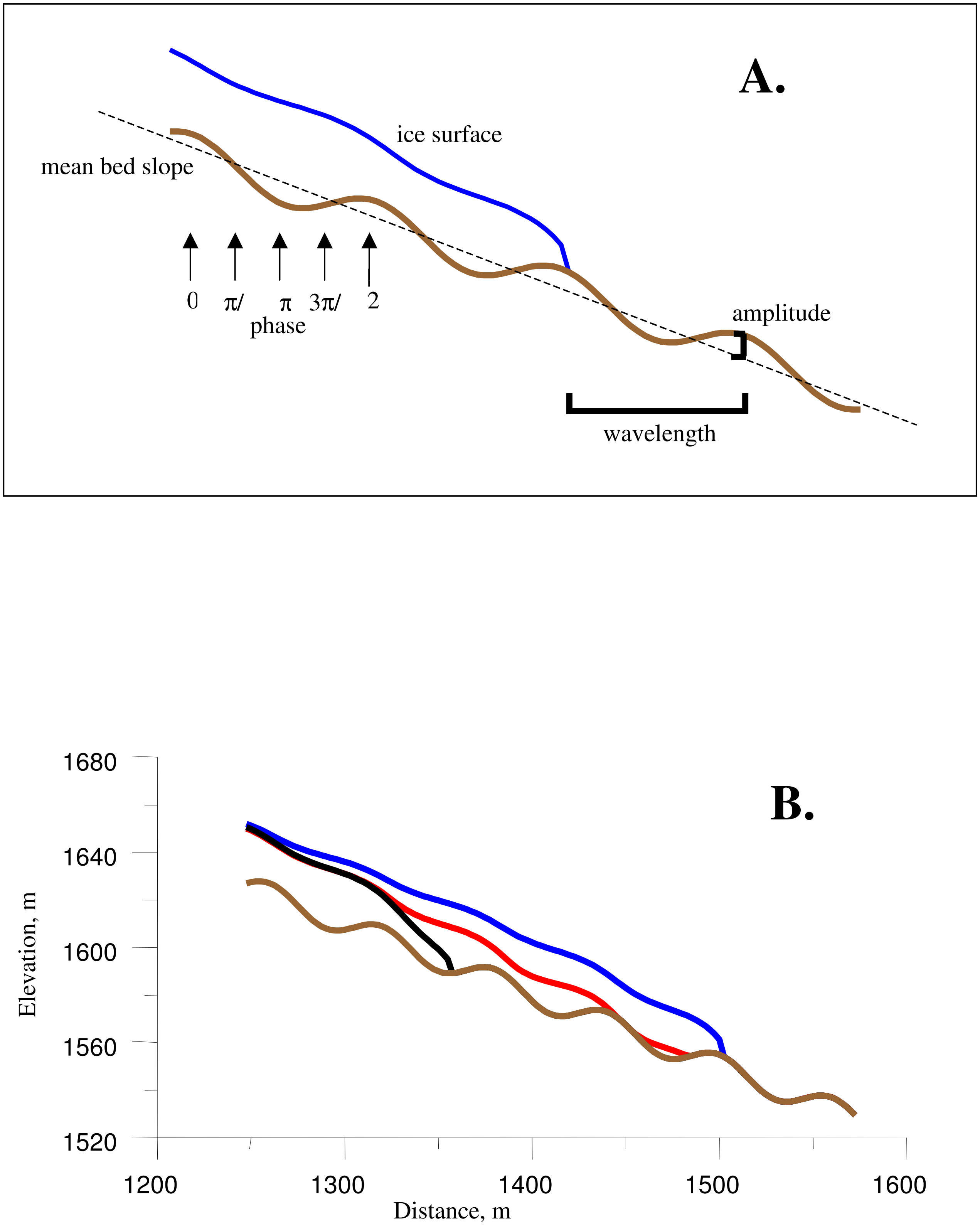

Figure 2.2 (A.) Profile of the model domain set up, showing bed (solid brown line) represented as a mean slope with a single cosine superimposed on it, ice (solid blue line), and mean bed slope (dashed line). The bed parameters that were varied are labeled: cosine wavelength, cosine amplitude, and cosine phase at the glacier head. (B) Glacial profiles showing the bed (brown), intitial steady state ice profile (blue), a profile during a stagnation event (red), and final steady state profile (black).

Results

Our model runs to steady state for generating initial conditions exhibit generally expected behavior. The location of the terminus is primarily controlled by the climatic setting (ELA elevation, snowfall rate, and PDD parameterization). As noted above, these were held constant at values taken from the literature (PDD parameterization) or tuned (ELA elevation versus snowfall rate) to simulate realistic glaciers within the model domain. The mean bed slope affects the glacier length; for specified elevation of the glacier head and the ELA, a steeper mean bed slope generates a shorter accumulation zone and a correspondingly shorter ablation zone. The terminus position is not strongly controlled by the sine-wave topography in our experiments, as revealed by a nearly uniform distribution of terminal phase locations.

Response to Instantaneous Warming (ELA Rise)

Warming causes the retreat of a fully continuous glacier body in some cases, and the pinch-off of terminal ice blocks in others. An example of such a stagnation event is shown in Figure 2.2B (solid red line). Shorter wavelengths were more likely to undergo stagnation (Figure 2.3). No stagnation events were created for wavelengths of 6 km or greater within our parameter space, even with our maximum warming of 5.6 ^{o}C , equivalent to 700 m ELA rise. Stagnation was more likely with larger amplitude bumps, and the importance of amplitude in causing stagnation increased with increasing wavelength. Because the thinnest sections of ice typically occurred over the crest of a bump (cosine phase ~0 radians), ice blocks were most likely to separate from the glacier on the down-glacier side of a bump, from phases of $\pi/2$ to π on the cosine.

Stronger warming events were more likely to force glacial stagnation (Figure 2.4A), suggesting that occurrence of a stagnation deposit can be used as a climate proxy. Increased warming drives faster down-wasting and melt back. Steeper bed slopes were less likely to stagnate (Figure 2.4B). This relationship has been investigated in other studies (Oerlemans, 2003), and the results agree. This relationship may also reflect the greater obstructive effect of given-amplitude bumps on flatter beds. Additionally, on flatter bed slopes, a given warming changes the glacier length more (Figure 2.5).

For a fixed bed slope, the stagnation length (the distance from the most upglacier point of pinch off to the original terminus) increases with increasing bed amplitude, and decreases with increasing wavelength (Figure 2.6A). For a fixed warming, the stagnation length increases with decreasing wavelength, as multiple pinch off blocks form over the rough bed. And, for a fixed wavelength and amplitude, stagnation length increases with increasing warming magnitude, and decreases with increasing slope (Figure 2.6B).

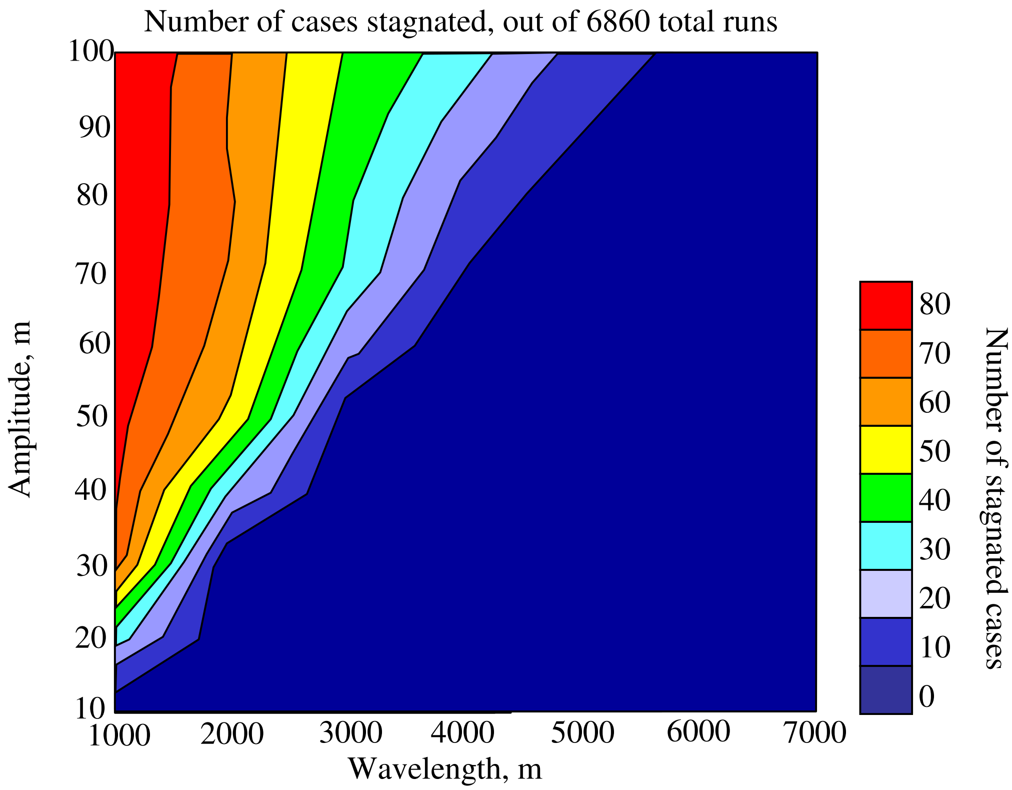

Figure 2.3. Contour plot showing the number of stagnating cases plotted over cosine wavelength (horizontal axis), and cosine amplitude (vertical axis). The results indicate that short wavelengths have a stronger influence on stagnation than high amplitudes (at the scale of our experiments).

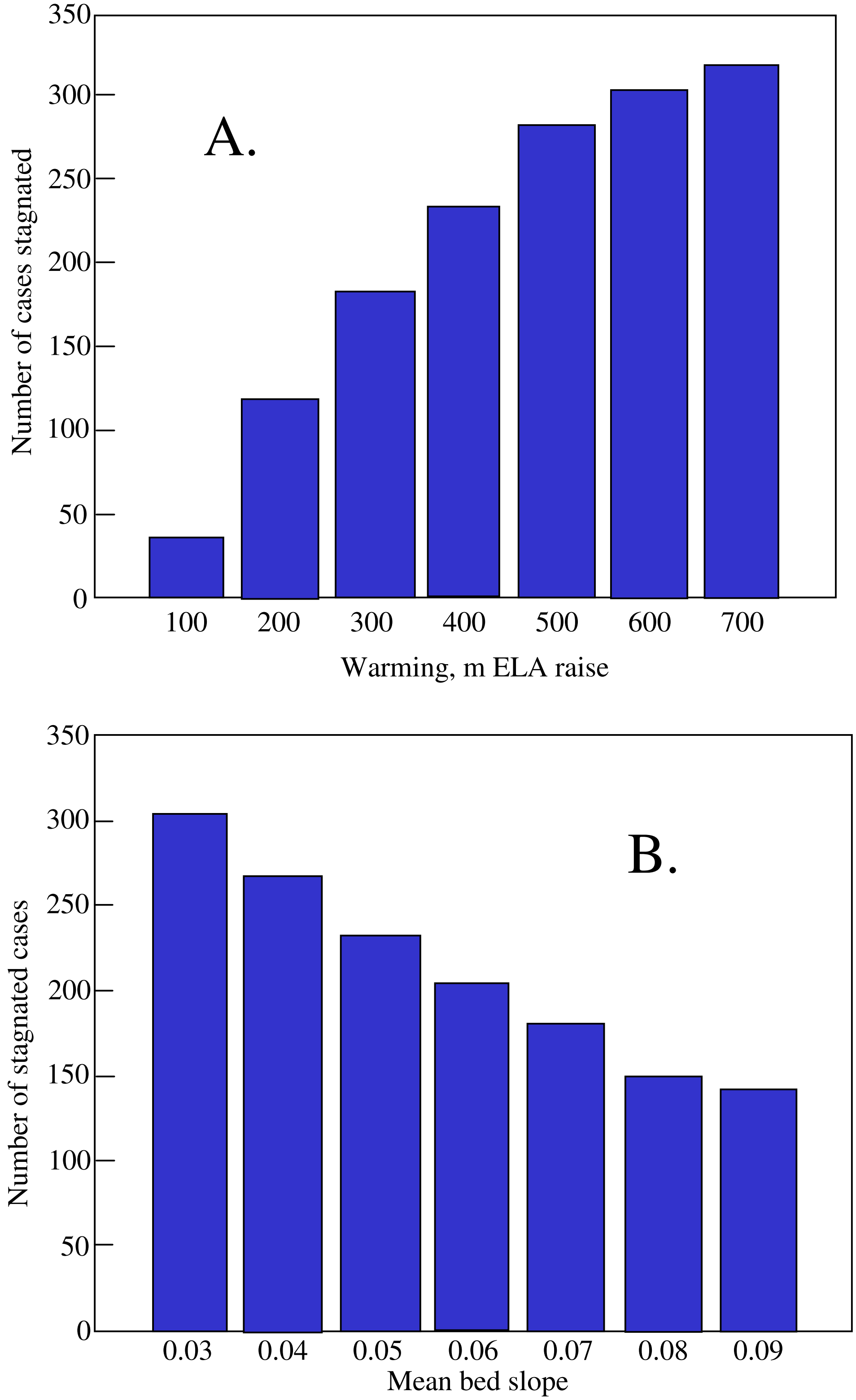

Figure 2.4. Histograms showing (A) the number of stagnating cases grouped by warming magnitude, and (B) number of stagnating cases grouped by mean bed slope. A total of 6860 runs were made.

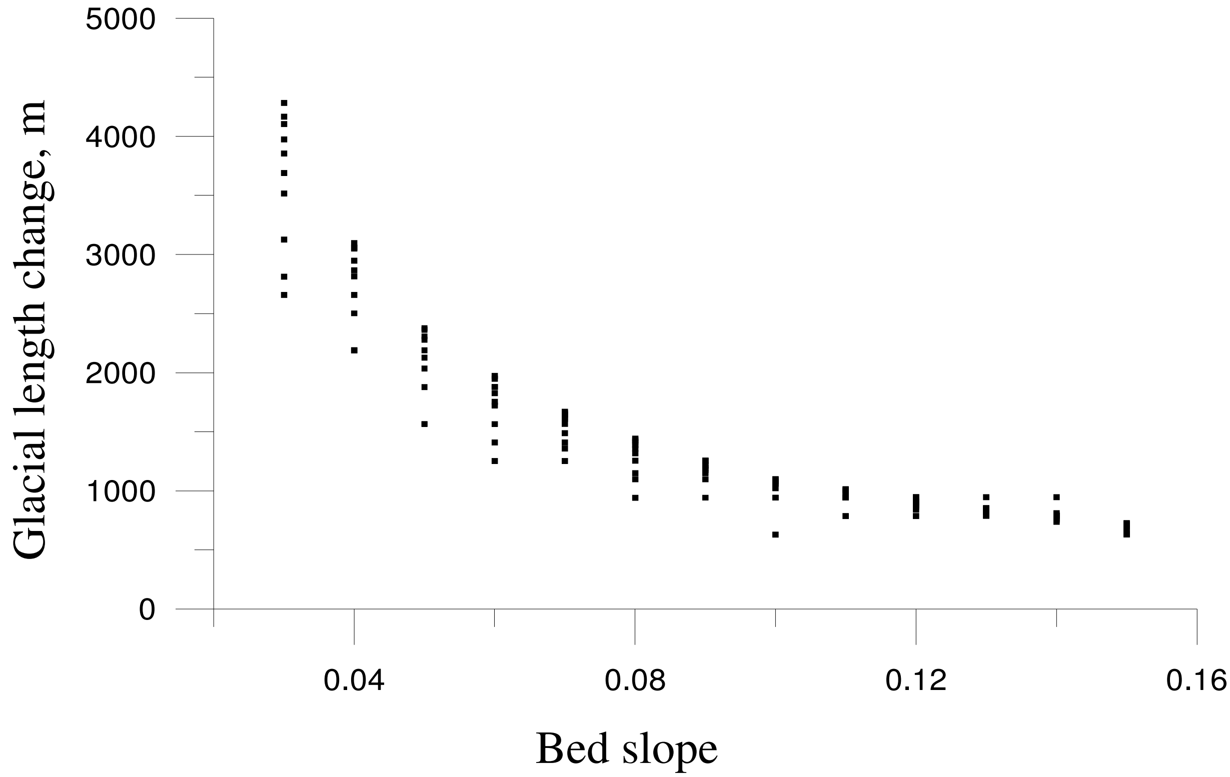

Figure 2.5. Plot of glacial length change over mean bed slope, for flat beds without superimposed cosine, over the range of warmings used in these experiments. The results indicate an inverse relationship between mean bed slope and glacial length sensitivity, given equal warming magnitude. The multiple data points for a given bed slope represent multiple warming magnitudes that were run.

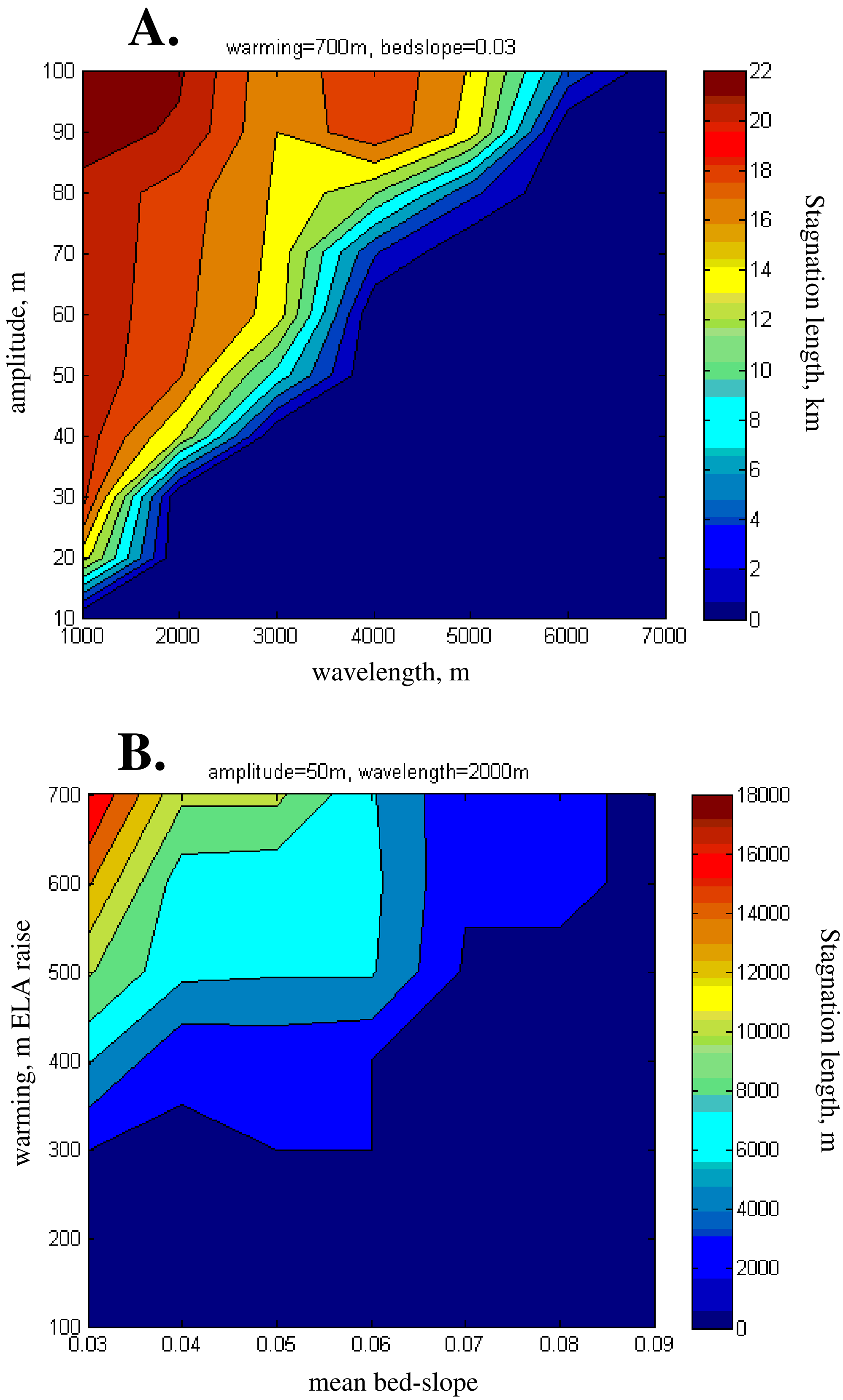

Figure 2.6. (A) Contour plot of stagnation length by amplitude and wavelength on the cosine, with fixed magnitude of warming and bed slope. (B) Contour plot of stagnation length by warming magnitude and slope, with fixed amplitude and wavelength.

The experiments described above were forced by instantaneous warming events of various magnitudes. Additional insight is provided by our experiments with variable-rate warming of fixed magnitude. As expected, the rate of warming did not affect the steady state length change. At warming rates slower than ~3.6 m/yr of ELA rise, no stagnation events occurred (Figure 2.7). For rates greater than 6.5 m/yr of warming, the length of stagnation was constant at 11,000 m (11 wavelengths), equivalent to the value for an instantaneous warming. In the range 3.6 to 6.5 m/yr of warming, stagnation length increased with increasing rate of warming (Figure 2.7).

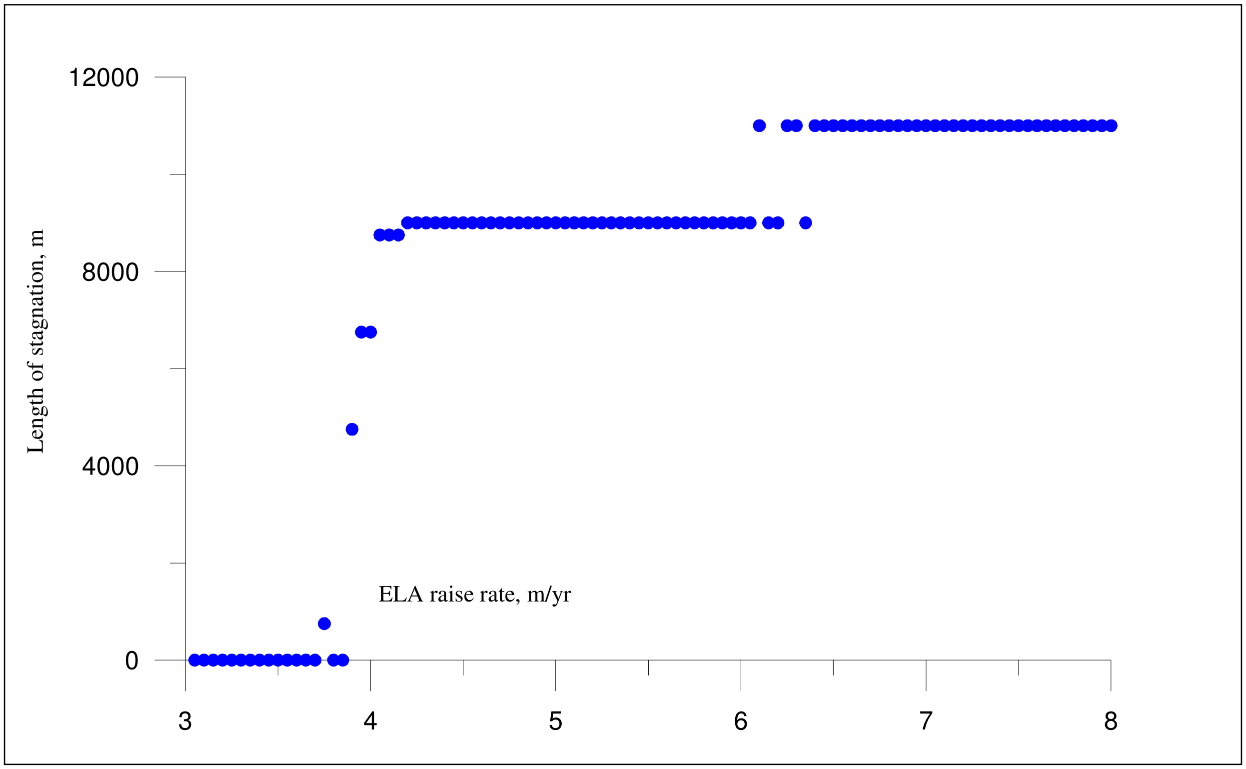

Figure 2.7. Stagnation length plotted over the rate of ELA raise per year. The bed parameters were: cosine wavelength = 1000 m, amplitude = 50 m, mean bed slope = 0.03, and the total ELA raise = 400 m. The results indicate that stagnation occurrence and magnitude is effected by the rate of warming, where greater warmings create larger stagnation events.

Discussion and Implications

Topographic Control

Our results show strong control of glacial stagnation by valley topography, confirming the results of Small (1995). Rougher beds (those with shorter wavelengths and higher amplitudes) are more likely to cause glacier stagnation (Figure 2.3). Within our range of parameters, most of the output variability was controlled by wavelength rather than amplitude.

Our experiments show that flatter mean valley slope is more likely to induce glacier stagnation (Figure 2.4B). Firstly, as noted by Small (1995), a glacier in a valley with a smaller mean slope loses more accumulation area for a given rise in ELA. Secondly, the superimposed cosine on the bed has greater local relief, causing more obstruction of flow, at least in the case of smaller bed slopes.

Stagnation as a climate proxy

For a given sinusoidal bed, events with larger or faster warming are more likely to cause stagnation. This is the basis for the potential use of presence or absence of stagnation deposits as a climate proxy; presence of stagnation deposits implies forcing by a minimum threshold of warming over time (Figure 2.6A-B). Warming triggers a twofold response in the glacier: melt back of the terminus, and down-wasting in the ablation zone. The onset of stagnation requires that down-wasting causes the local ice to melt entirely before the terminus retreats through the down-wasting region. In a typical valley glacier, the process of vertical down-wasting has O(100 m) of ice to melt, whereas the scale of horizontal melt-back of the terminus to reach the same location is O(10 km).

Thus stagnation is favored by larger warming or by faster warming; sufficiently slow climatic warming can be large without forcing stagnation. In our results, a critical threshold rate of climatic warming existed below which stagnation did not occur. Above that rate, the length of glacier tongue that stagnated increased as the rate of warming increased, up to a limit beyond which the warming was essentially instantaneous and the results became independent of rate (Figure 2.7). Thus, occurrence of stagnation deposits implies instantaneous climatic warming of some specific magnitude, or a larger but slower warming, as discussed below.

Limitations of our assumptions

In our simulations, we defined glacial stagnation to occur only if a terminal block of ice pinched off from the main glacial body. As shown in our modeling, conditions are possible in which ice remains attached to the main glacier but slows essentially to zero. There is, in principle, no difficulty in tracking ice velocity as a function of time at all nodes, and in searching for such situations; we took the simpler approach for this study, but would recommend the more complete approach in any model focused on obtaining quantitative results for a given bed configuration (see Vacco, 2009, chapter 3 for an example).

We anticipate that some iteration may be required between glacial geology and ice-flow modeling to realize the full potential for paleoclimatic reconstruction from presence/absence of stagnation deposits. In particular, stagnation deposits developed by ice with abundant supraglacial debris are easily identified, but less attention has been focused on the possibility of stagnation of "clean" ice leaving little geologic trace. We suspect that usually there are indications of such situations, but suggest that more study may be needed. The length over which a glacier stagnated in our models increases with magnitude or rate of climatic warming. Recognizing whether a region of stagnation deposits represents a single warming event, or multiple but smaller warming events, may take careful fieldwork, as may identifying cases where the ice retreated for some distance and then stagnated.

For this study we wanted to isolate the simplest case of glacier flow, applying a model containing internal deformation of ice with no other dynamic processes. Real glaciers may include additional stresses, basal sliding or till deformation, basal melting, and other processes or influences. Modeling full stresses will more accurately simulate the reality that ice is to some extent "shoved" over bumps (longitudinal stress coupling) without as much thinning as in the shallow-ice approximation, reducing the tendency for stagnation. Including till deformation or basal sliding lubricated by basal melting will make the modeled ice thinner, favoring stagnation. A model addressing a particular glacier ideally would include the relevant processes, and be tuned to match the pre-retreat situation.

The biggest mechanism to be addressed is the effect of debris cover on glacial retreat. Sufficiently thick debris is notably reduces surface melting, allowing a glacier to extend farther down-glacier, and to have more of its area below the ELA, than for a "clean" glacer (e.g., de Sassure, 1786; Deline and Kirkbride, 2009). In turn, this favors occurrence of stagnation following warming, aided by the generally concave-up form of mountain valleys such that a longer glacier often reaches a region of lower bed slope. We have not included simulations with varying debris cover in this paper, in part because of the number of complex issues raised related to poor knowledge of sources, concentrations, and effective thermal influence in light of supraglacial redistribution processes (Vacco, 2009, chapter 3, and Vacco et al., in preparation). Our experiments indicate that basal topography can cause stagnation with no debris present on the ice surface. Glaciers resting on rougher beds with flatter mean slopes, or subjected to faster or larger warming, are more likely to stagnate.

We have not yet generated a fully quantitative paleoclimatic tool. However, we see no fundamental difficulties in doing so. The presence or absence of stagnation deposits from glaciers tied to dated moraines can be recognized in the field, and correlated across numerous adjacent valleys with diverse topography. For any one glacier, a flow model can be developed to match extent, thickness from trim lines, etc., taking account of topography and any available information on climate, debris cover, debris supply and basal lubrication. Subjecting this model to varying sizes and rates of warming can then map out the thresholds for occurrence of various stagnation lengths.

Comparison to the observed absence, or presence and length, of stagnation indicators then should place limits on the climatic change responsible for the glacier retreat. In the absence of stagnation deposits, the warming must have been slower or smaller than the calculated threshold. In the presence of stagnation deposits of specific length, the warming must have been larger and faster than the threshold, with some tradeoff between the size and rate. Repeating this exercise for several nearby valleys with different stagnation features should then provide rather tight constraints on the climate change. We do not yet know whether this can be done with sufficiently small uncertainties to be paleoclimatically useful, but the prospect is intriguing.

Conclusions and Future Work

Our simple glacier-model results show that, in response to warming, stagnation of part of the terminal region of a glacier is more likely given: (A) more warming, (B) flatter mean bed slope, (C) shorter sinusoidal wavelength, (D) higher sinusoidal amplitude, (E) faster rate of warming, and/or (F) thinner ice.

These results imply that estimates of rate or magnitude of warming are possible from the existence and extent of observed stagnation terranes. To do this, one would use glacial-geological evidence of moraines and trim lines to reconstruct the extent and thickness of the pre-warming glacier on the topography. Additional input would be needed in terms of the climate that supported the pre-warming glacier, although the usual relations between elevation and temperature, and between accumulation-area and ablation-area on a glacier, may prove sufficient (Oerlemans, 2001). For instance, the presence of a dated end moraine, plus the relation between accumulation and ablation areas, allows reconstruction of snowlines and thus temperatures before a warming event (Oerlemans 2001; Denton et al., 2005). Knowledge of soft-bedded or hard-bedded conditions would guide specification of basal sliding/bed deformation in the model, with tuning to match the pre-warming configuration. In this way, the topographic and other aspects described by Small (1995) and in our modeling above could be specified.

Once the bed configuration is known, different rates and magnitudes of warming can be applied to the glacier model, and the modeled presence/absence and extent of stagnation deposits compared to those observed. Our model results indicate that sufficiently small or slow climatic warming would cause no stagnation, and so would be excluded by the presence of stagnation deposits in the field. Sufficiently fast climatic warming would appear instantaneous to the glacier, in which case the length of stagnation would be controlled by the magnitude of the warming event. For intermediate magnitudes of climatic warming events, some tradeoff will exist such that larger and slower or smaller and faster warming will be consistent with the observed stagnation deposits, so unique results may not be available. However, if multiple glaciers in a region can be studied, the tradeoff is likely to be different on different glaciers, allowing a unique determination to be made.

In summary, our results show that the presence or absence of stagnation deposits, and the extent of such deposits, allow quantitative limits to be placed on the size or rate of warming involved in forcing retreat from the moraine, providing additional useful paleoclimatic information.

Acknowledgements

We thank Patrick Applegate, Rudy Slingerland, Byron Parizek and Sridhar Anandakrishnan for helpful discussions, and three anonymous reviewers for comments that significantly improved the manuscript. For partial support, we thank the US National Science Foundation (under grants 0531211, 0539578 and 0424589), and the Comer Science and Education Foundation.

References

Boone, S. J., and Eyles, N. (2001). Geotechnical model for Great Plains hummocky moraine formed by till deformation below stagnant ice. Geomorphology **38**(1-2): 109-124.

Braun, D. D. (2006). Deglaciation of the Appalachian Plateau, northeastern Pennsylvania--till shadows, till knobs forming "beaded valleys": Revisiting systematic stagnation-zone retreat. Geomorphology **75**: 248-265.

Brown, D. G., Lusch, D. P., and Duda, K. A. (1998). Supervised classification of types of glaciated landscapes using digital elevation data. Geomorphology **21**: 233-250.

Budd, W. F. (1968). The longitudinal velocity profile of large ice masses. International Association of Scientific Hydrology--Association Internationale d'Hydrologie Scientifique (International Union of Geodesy and Geophysics--Union de Geodesie et de Geophysique Internationale), Publication. (79): 58-77.

Clarke, G. K. C. (1976). Thermal regulation of glacier surging. Journal of Glaciology **16**(74): 231-250.

Clayton, L. (1964). Karst topography on stagnant glaciers. Journal of Glaciology **5**: 625-656.

Clebnik, S. M., and Mulholland, J. W. (1979). Regional stagnation of ice in northeastern Connecticut: An alternative model of deglaciation for part of New England: Discussion and reply. Geological Society of America Bulletin **90**: 117-120.

de Saussure,H.-B.,1786. Voyages dans les Alpes, Précédés d'un Essai sur l'HistoireNaturelle des Environs de Genève. Tome second. Barde, Manguet & Compagnie. Genève

Deline, P., and Kirkbride, M. P., 2009, Rock avalanches on a glacier and morainic complex in Haut Val Ferret (Mont Blanc Massif, Italy). *Geomorphology* 103, p. 80-92.

Denton, G. H., Alley, R. B., Comer, G. C., Broecker, W. S. (2005). The role of seasonality in abrupt climate change. Quaternary Science Reviews **24**: 1159-1182.

Eyles, N., Boyce, J. I., and Barendregt, R. W. (1999). Hummocky moraine; sedimentary record of stagnant Laurentide ice sheet lobes resting on soft beds. Sedimentary Geology **123**(3-4): 163-174.

Gravenor, C. P., and Kupsch, W. O. (1959). Ice-disintegration features in western Canada. Journal of Geology **67**: 48-64.

Ham, N. R., and Mickelson, D. M. (1994). Basal till fabric and deposition and Burroughs Glacier, Glacier Bay, Alaska. Geological Society of America Bulletin **106**: 1552-1559.

Haselton, G. M. (1966). Glacial geology of Muir Inlet, southeast Alaska. Institute of Polar Studies Report, Ohio State University. **18**.

Hutter, K. (1983). Theoretical Glaciology; material science of ice and the mechanics of glaciers and ice sheets. Tokyo, D. Reidel Publishing Co.

Huybrechts, P., Payne, A. J., and EISMINT Intercomparison Group (1996), The EISMINT benchmarks for testing ice-sheet models. Annals of Glaciology 23, 1-12.

Johnson, M. D., Mickelson, D. M., Clayton, L., Attig, J.W. (1995). Composition and genesis of glacial hummocks, western Wisconsin, USA. Boreas **24**(2): 97-116.

Kamb, B., Echelmeyer, K. A. (1986), Stress-gradient coupling in glacier flow. 1. Longitudinal averaging of the influence of ice thickness and surface slope. Journal of Glaciology **32**(111), 267-284.

Kopczynski, S. (2008), Satellite Predictions of Subglacial Hydrology Transitions, and Final Ice Collapse of the Anchorage Lowland, Alaska. PhD Thesis, Lehigh University, Bethlehem, PA, USA.

LeMeur, E., Gagliardini, O., Zwinger, T., Ruokolainen, J., 2004, Glacier flow modelling: a comparison of the shallow ice approximation and the full-Stokes solution. Comptes Rendus Physique 5, 709-722.

Mannerfelt, C. M. (1961). Stagnation or activity in the last ice remnants? Geografiska Annaler **63**(3-4): 139-147.

McKenzie, G. D. (1970). Glacial geology of the Adams Inlet. Institute of Polar Studies Report, Ohio State University. **25**.

Mickelson, D. M. (1971). Glacial geology of the Burroughs Glacier area, southeastern Alaska. Institute of Polar Studies Report, Ohio State University. **40**.

Oerlemans, J. (2001). Glaciers and Climate Change. Lisse / Abingdon / Exton (PA) / Tokyo, A.A. Balkema Publishers.

Oerlemans, J. (2003). A quasi-analytical ice-sheet model for climate studies. Nonlinear Processes in Geophysics **10**(4/5): 441-452.

Pattyn, F. (2002). Transient glacier response with a higher-order numerical ice-flow model. Journal of Glaciology **48**(162): 467-477.

Paul, M. A., and Eyles, N. (1990). Constraints on the preservation of diamict facies (melt-out tills) at the margins of stagnant glaciers. Quaternary Science Reviews **9**: 51-69.

Sharp, R. P. (1988). Living ice. Understanding glaciers and glaciation, Cambridge University Press.

Small, E. E. (1995). Hypsometric forcing of stagnant ice margins: Pleistocene valley glaciers, San Juan Mountains, Colorado. Geomorphology **14**: 109-121.

Tuthill, S. J. (1966). Earthquake origin of superglacial drift on the glaciers of the Martin River area, south-central Alaska. Journal of Glaciology **6**(43): 83-88.

Vacco, D. A., 2009, Modeling of glacier response to climate change, including moraine deposition and stagnation events: Doctoral Dissertation. Department of Geosciences, Pennsylvania State University.

van der Veen, C. J. (1999). Fundamentals of Glacier Dynamics. Rotterdam, Balkema.

CHAPTER 3. MODELING SUPRA-GLACIAL DEBRIS

3.0 Introduction

Chapter 3 contains three sections.

Section 3.1 is the manuscript I am preparing for submission to *Geophysical Research Letters*. This manuscript addresses an issue of timely importance, and so is a short paper to be published rapidly. My modeling results show that rock avalanches deposited on glaciers trigger glacial advance followed by stagnation, in the absence of climate change. As described in section 3.1, recent papers have argued that the Waiho Loop, New Zealand, was created by an avalanche onto the Franz Josef Glacier. My supraglacial modeling results indicate that it is very unlikely that an avalanche caused the deposition of the Waiho Loop.

Section 3.2 contains a much broader range of supraglacial modeling experiments, involving sources of debris other than avalanches, and climate changes. These results will be submitted as a longer paper in the near future.

Section 3.3 is a summary of the supraglacial modeling studies, including future work.

3.1 In prep, to be submitted to *Geophysical Research Letters*: Effect of Rock Avalanches and Supraglacial Debris on Glaciers

Authors:
David A. Vacco
Richard B. Alley
David Pollard

3.1.0. Abstract

Rock avalanches that are deposited on glaciers and that are large enough to cause glacier advances will lead to extended, hummocky deposits rather than discrete moraine ridges, based on results of ice-flow modeling. Sufficiently thick supraglacial debris in ablation zones reduces the ice surface melting significantly. When a discrete, extensive body of debris (a landslide) is introduced to a debris-free glacier surface, the model glacier advances until the upglacier end of the debris cover passes the previous terminus, followed by formation of a terminal stagnation lobe. The section of ice that advanced beyond the original terminus slowly thins, ceases flowing and melts in place, eventually returning the glacier profile to its original shape.

3.1.1. Introduction

Rock avalanches and supraglacial debris are known to affect glacier mass balance and terminus dynamics. In particular, rock avalanches deposited on glaciers have been observed to trigger glacial advance (Hewitt, 2009; Deline and Kirkbride, 2009; also see

McSaveney, 1978; Larsen et al., 2005, D'Agata 2005). As noted by Deline and Kirkbride (2009), both de Saussure (1786) and Agassiz (1845) attributed glacier advance to the insulating effect of thick debris cover deposited by landslide.

Glacial deposits are widely and successfully used as paleoclimatic indicators, with cooling or increased snowfall causing advances. Cosmogenic dating of glacial deposits has been very successful in interpreting glacial history. Such interpretation requires that field workers are able to distinguish climatically triggered advances from those forced by landslide deposition.

Investigators often link supraglacial landslide deposition to production of horizontally extensive deposits with a hummocky character (see Deline and Kirkbride (2009) and references therein). This is based on a conceptual model in which the thick and extensive debris cover of a landslide greatly reduces surface ablation, allowing the ice bearing the slide mass to advance beyond the original terminus of the glacier. Stagnation or near-stagnation then follows, with slow downwasting producing thermokarst features that generate the hummocky topography.

However, a recent study (Tovar et al., 2009) interpreted the prominent single moraine ridge of the Waiho Loop, Franz Josef Glacier, New Zealand, as the deposit resulting from a glacier advance triggered by a supraglacial landslide. Angularity of debris, and absence of striations and polish, indicate supraglacial or englacial rather than subglacial transport, and relative homogeneity of lithology is suggested to occur and to indicate a landslide origin. The Waiho Loop has previously been argued to record an important climatic change (Denton and Hendy, 1994). This raises an interesting debate.

In this contribution, we use a physical ice-flow model including supraglacial debris transport and its shielding of glacial melting to provide insight to the ice-flow response to supraglacial landslide deposition, and the resulting landslide deposits following ice melting. The model indicates that a supraglacial landslide capable of triggering a significant glacial advance will produce a laterally extensive deposit as a result of a stagnation event.

3.1.2. Thermal influence of supraglacial debris

Many studies have investigated the effects of debris cover on glacial melting (Anderson, 2000; Mattson, 2000; Pelto, 2000; Conway and Rasmussen, 2000; Haidong et al., 2006). Although supraglacial material in small amounts increases melting (e.g., Hansen and Nazarenko, 2004; Conway et al., 1996), notable debris cover primarily serves to insulate the glacier surface from atmospheric energy fluxes, reducing melting. For a uniform debris layer, the effect can be approximated by an exponential decrease in melting with increasing debris thickness, with an e-folding length of ~0.1 m (Anderson 2000).

Observations show that debris cover often is not uniform, but instead is redistributed by small-scale processes. For example, the toe of the Tasman Glacier, New Zealand, is covered in a layer of debris averaging 1 – 2 m thick but with important spatial variability (Hochstein et al., 1995, Schomacker, 2008). Development of supraglacial lakes, collapse features, and other "thermokarst" features has caused debris redistribution, so that bare ice is visible in some places. The ice surface has been lowering ~1 m/year (Hochstein et al., 1995), far faster than would be expected solely from surface melting in response to meteorologic energy fluxes, but more than an order of magnitude slower than expected for equivalent clean ice (Kirkbride, 1995). A 15-fold reduction in melting from a 1.5-m-thick debris layer implies an effective thermal e-folding length of 0.6 m. The debris cover has contributed to stagnation/isolation of some ice in the terminal region, which overall is near stagnant with ice flow velocities < 4.0 m/yr.

We know of no fully calibrated process models for the local debris redistribution and other processes that reduce but do not eliminate the insulating effect of supraglacial debris layers. As a first parameterization, we simply test changes in the e-folding length for the thermal effects of the debris.

3.1.3. Supraglacial debris model

The insulating effects of a debris layer are thus treated through the melt-rate parameterization:

$$\dot{m}_r = \dot{m}\exp\left(\frac{-h_r}{H_r*}\right) \qquad (3.1.1)$$

where $\dot{m}$ = the melt rate of bare ice in m/yr, h_r = the debris layer thickness, H_r* = the e-folding thickness = 0.1 m or some larger chosen value, and $\dot{m}_r$ = the melt rate with debris cover (Anderson, 2000).

Supraglacial debris is advected with the ice-surface velocity, and also affected by mass-movement processes. Following widespread practice in geomorphology, we treat the mass-movement term diffusively. Including these processes, we get the supraglacial debris equation:

$$\frac{\partial h_r}{\partial t} = k\frac{\partial^2 s_r}{\partial x^2} - \frac{\partial}{\partial x}\left(h_r u_i\left(s_i\right)\right) + D \qquad (3.1.2)$$

where h_r = thickness of supraglacial debris in meters, s_i = the ice surface elevation, $u_i(s_i)$ = ice velocity at the ice surface in m/yr, s_r = the supraglacial debris surface elevation, k = the mass diffusivity of debris in m^2/yr, and D = mass source of debris in m/yr. We have built a general version of this model in which the source term D includes the melt-out of englacial debris, proportional to the debris concentration in the ice and the surface melt rate, with the debris concentration tunable to reflect relative importance of headwalls, rates of mass wasting there, etc. For this study, we apply individual landslides at discrete intervals as the source of debris mass to the system.

Mass wasting of supraglacial debris has not been studied extensively. For general unconsolidated sediment, mass wasting is often modeled as a diffusive process (Martin, 2000; Hanks, 2000), and we follow this approach. We start with a diffusivity of k = 0.1 m^2/yr, relatively large compared to hillslope diffusion and fault scarp development, and slightly larger than the effective diffusivity of k = 0.03 m^2/yr obtained by Anderson (2000) for the thin (~5-cm) supraglacial debris melting out of medial moraines. In light of the considerable uncertainties, we tested order-of-magnitude and larger changes in diffusivity. With advective ice flow velocities typically of order 10-100 m/yr, our results are insensitive to diffusivity for values less than order of 100 m^2/yr.

To compute ice flow, we apply the shallow ice approximation:

$$\frac{\partial H}{\partial t} = \frac{\partial}{\partial x}\left[A' H^{n+2} \left| \frac{\partial s_i}{\partial x} \right|^{n-1} \frac{\partial s_i}{\partial x} \right] + \dot{b}(z,t) \qquad (3.1.3)$$

where $\dot{b}(z,t)$ = the local surface mass balance of ice in m/yr, H = local ice thickness in meters, $A' = A(\rho_i g)^n$, where A = ice softness = 6.8 x 10^{-15} Pa^{-3} yr^{-1}, the stress exponent n = 3, ρ_i = ice density = 920 kg/m^3, and g = acceleration due to gravity = 9.81 m/s^2. We assume the glacier to be sliding at the base, using the sliding law:

$$u_b = B\tau_b^m \qquad (3.1.4)$$

where u_b = basal ice velocity, m/yr, τ_b = basal shear stress, B = sliding law coefficient = 0.05 m Pa^{-2} yr^{-1} (chosen to give reasonable sliding velocities) and the sliding exponent m = 2.

Ablation is parameterized using the positive degree-day approach (PDD, Van der Veen, 1999), with a constant melting parameter of 0.008 m $^oC^{-1}$ day^{-1}. The seasonal temperature variation is approximated as a sine wave with amplitude 15 ^oC. The elevation lapse rate of temperature is assumed to be -0.008 ^oC m^{-1}. A uniform snowfall rate of 2.0 m yr^{-1} ice-equivalent is applied at all elevations.

3.1.4. Experiment Description

For the purpose of simulating supraglacial debris deposition by avalanching, we assume instantaneous delivery of sediment of specified length and uniform thickness to the glacier surface. Avalanche volumes are modeled to fall within ranges of observed landslide events on glacial surfaces (Hewitt, 2009).

The experiments are initialized by running the ice-flow model to steady state under constant climate conditions, with no supraglacial debris. Then sediment is instantly delivered to a specified region of the ice surface, and the model is run until a new steady state develops, while holding climate steady. Additional experiments, not reported in detail here, show that the effect of adding landslide debris is greatly reduced if substantial supraglacial debris is already present.

Most of our experiments have been conducted on a planar sloping bed of inclination 0.04, although we have also investigated other valley profiles. We primarily have investigated avalanche sizes of 1 – 5 km in length and 10 – 50 cm in thickness covering the ablation zone of the glacier (figure 3.1.1).

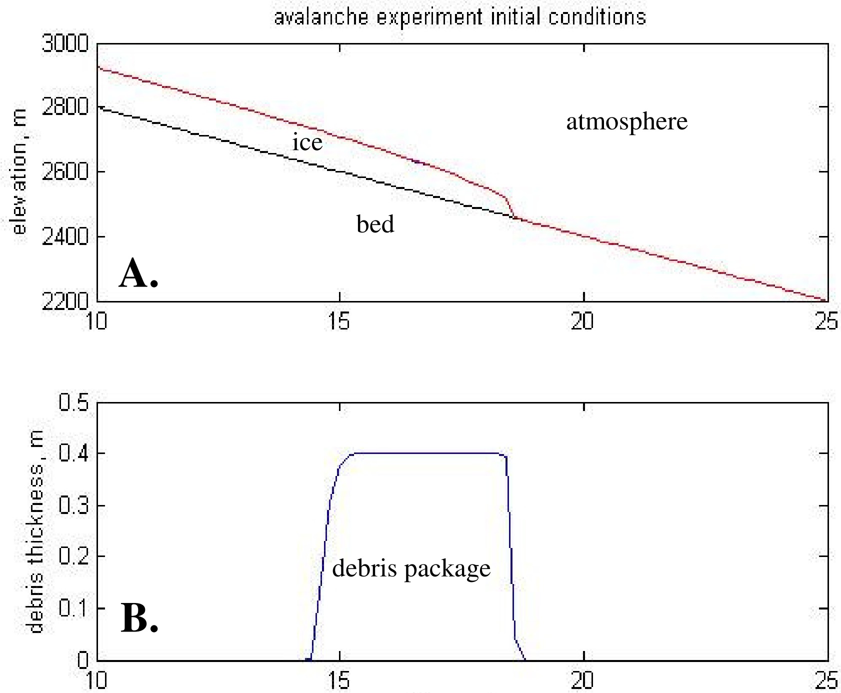

Figure 3.1.1. Avalanche experiment initial conditions (A) ice profile, and (B) supraglacial debris thickness. The debris package is introduced to the system instantaneously.

In order to investigate the possibility that avalanching had a role in the Waiho Loop deposition (Tovar et al., 2008), we run avalanche experiments on a 1-d profile, approximating the Franz Josef Glacier valley, New Zealand. The bed elevation is simplified to a planar, sloping surface, with two breaks in slope, similar to the actual valley topography (figure 3.1.2). Our simplified 1-d model makes no attempt to provide an exact match to the Franz Josef Glacier. Our leading results prove to be robust against order-of-magnitude changes in the leading parameters, so post facto the validity of modeling without an exact match is justified.

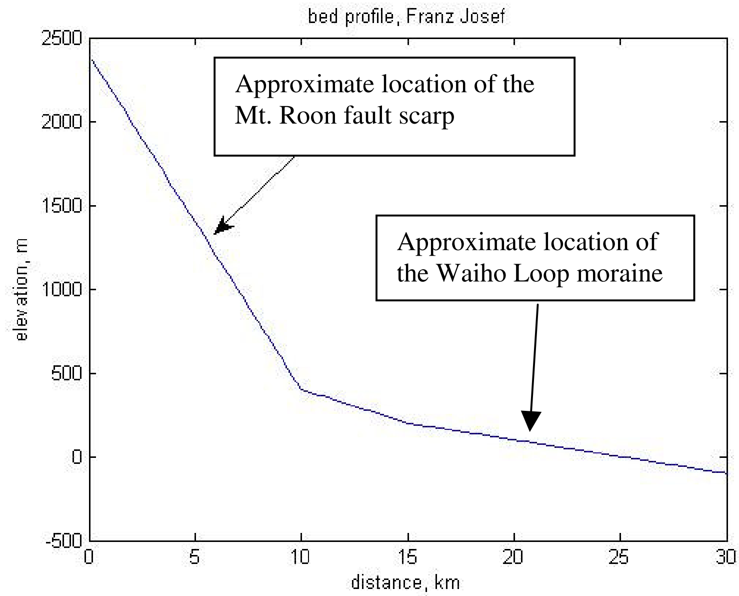

Figure 2. Glacial bed profile, modeled after the Franz Josef glacial valley, New Zealand.

The topography of the Waiho Loop indicates a volume of ~ 10^8 m^3 (Tovar, 2008). The Waiho Loop moraine has been eroded by streams, so modern measurements of the volume represent a minimum estimate of its volume at the time of deposition. The Franz Josef valley has an average width of 1 km; thus, a landslide of 10^5 m^2 per meter width would be required to supply the entire moraine. This is equivalent to a 10 m thick layer of sediment covering half of the ~ 20 km glacier length, measured from the glacier head to the Waiho Loop. As described below, a range of model experiments indicates that a moraine formed in response to a landslide-triggered advance will contain no more than ~20% of the landslide debris, and probably much less than 20%, so we require a minimum avalanche five times larger than the Waiho Loop (50 x 10^5 m^2). Thus, we deposit a 65 m thick avalanche layer on the glacier that is 7.7 km long beginning at the east face of Mt. Roon (Tovar (2008) hypothesized that the avalanche scarp on Mt. Roon may be the avalanche that caused deposition of the Waiho Loop).

3.1.5. Experiment results, avalanche effects on glacial dynamics

In all experiments, covering the ablation zone with enough supraglacial debris to significantly reduce melting triggered a glacial advance. Ice surface advection transports the avalanche down-valley as the glacier terminus advances, aided slightly by diffusive mass wasting of the sediment. Even the smallest avalanches tested (length 1 km, thickness = 0.05 m) caused a short advance followed by a stagnation event. The upglacial limit of the sediment package is transported down-valley of the original steady-state terminus. Then, the ice flux past the original terminus drops to zero. The extended, debris-covered ice down-wastes slowly in place, and eventually flow velocities approach zero. We term this a stagnation event. For this study, we define stagnation as the glacial state in which ice has a thickness greater than 10 m, and flow velocity less than 10 cm per year. We infer that the supraglacial debris would be dropped directly to the bed, producing hummocky stagnation deposits.

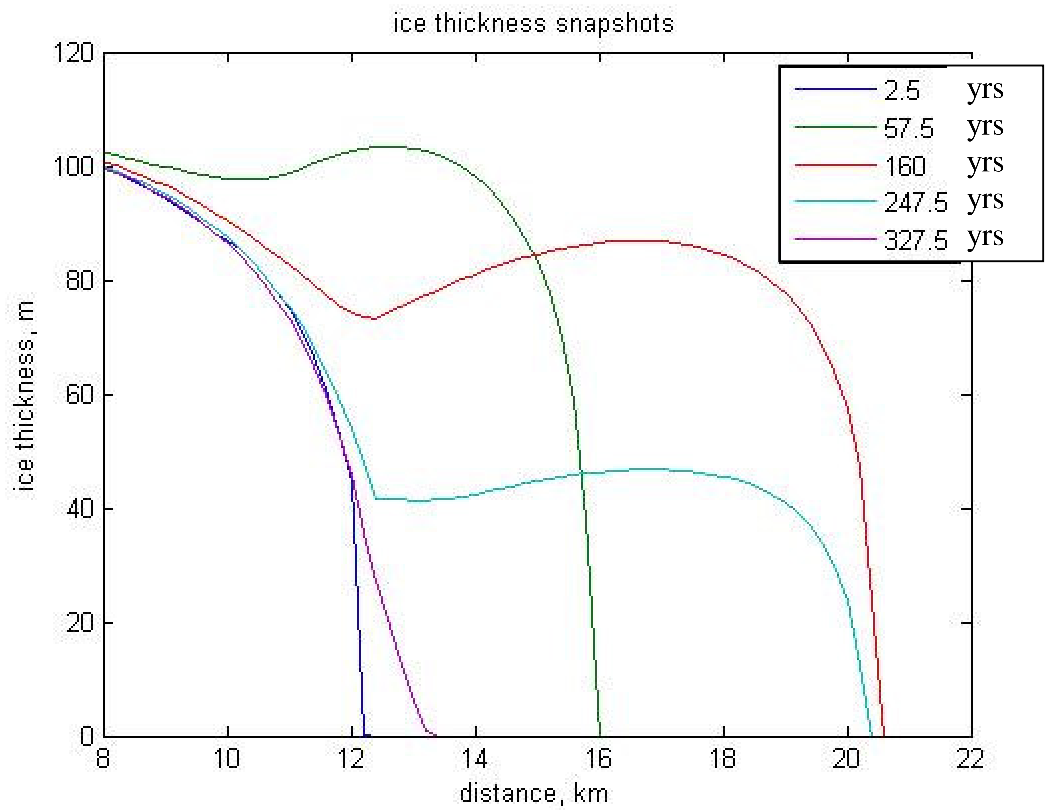

Figure 3.1.3. Snapshots of the ice thickness over time, after deposition of a 2 km long, 35 cm thick supraglacial debris layer.

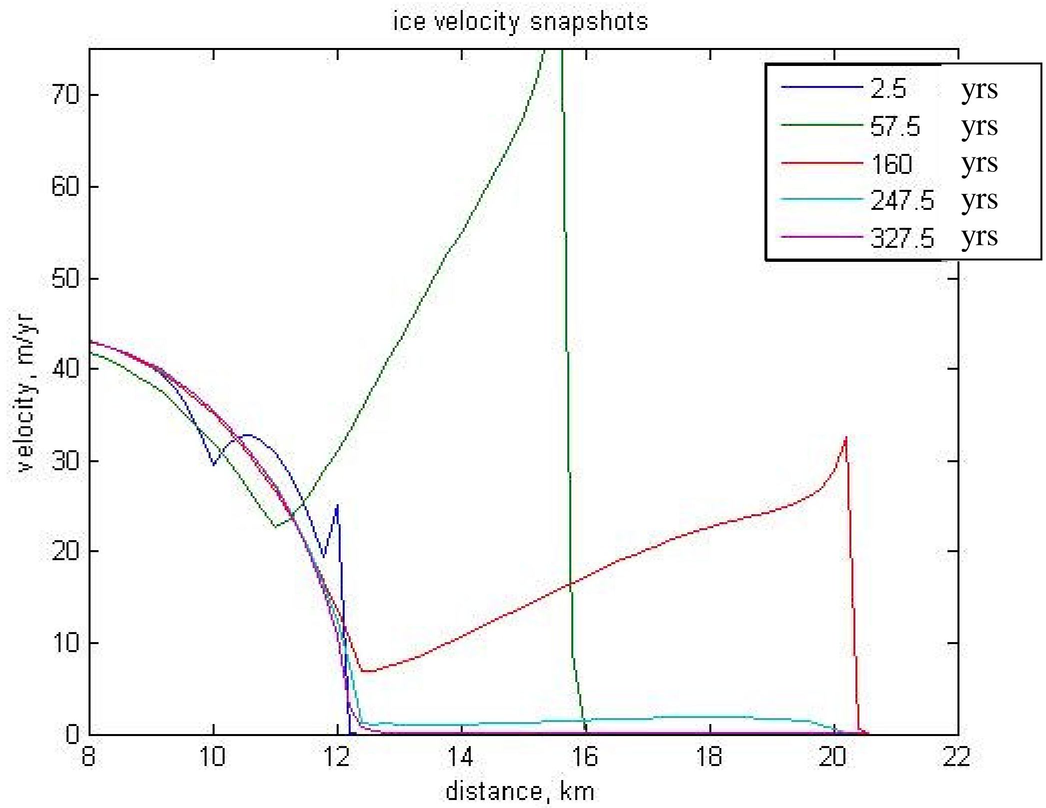

Figure 3.1.4. Snapshots of the ice velocity development over time, after deposition of a 2 km long, 35 cm thick supraglacial debris layer.

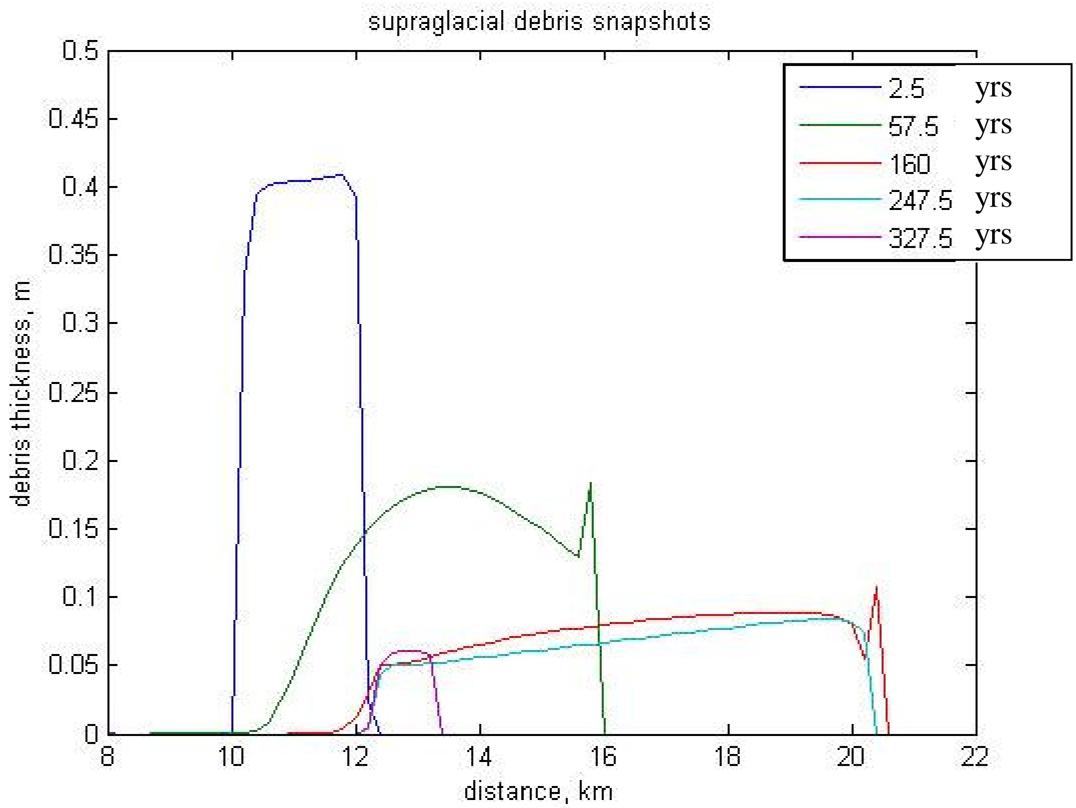

Figure 5. Snapshots of the supraglacial debris development over time, after deposition of a 2 km long, 35 cm thick supraglacial debris layer. Any sediment that is deposited to the bed is not plotted

The length of stagnation deposits produced depends on the thickness and length of the avalanche (figure 3.1.6). In the model, avalanches trigger stagnation fields that are roughly an order of magnitude longer than the initial avalanche length. The ice flow velocities are divergent within the advancing band of debris covered ice except very near the ice front (Figure 3.1.4), which leads to a significant amount of spreading of the supraglacial debris layer as the glacier terminus advances. (Analogy might be drawn between the advancing debris-covered ice and a drip of paint moving down a wall and then stopping.)

Longitudinally convergent flow very near the ice front (Figure 3.1.4) is associated with some thickening of supraglacial debris there (Figure 3.1.5). In addition, melting and mass-wasting there lead to transport of some sediment off the toe of the glacier. If all of the ice-front sediment is assumed to remain there to form a moraine, with zero removal by proglacial streams, roughly 20% of the original debris ends up in the moraine.

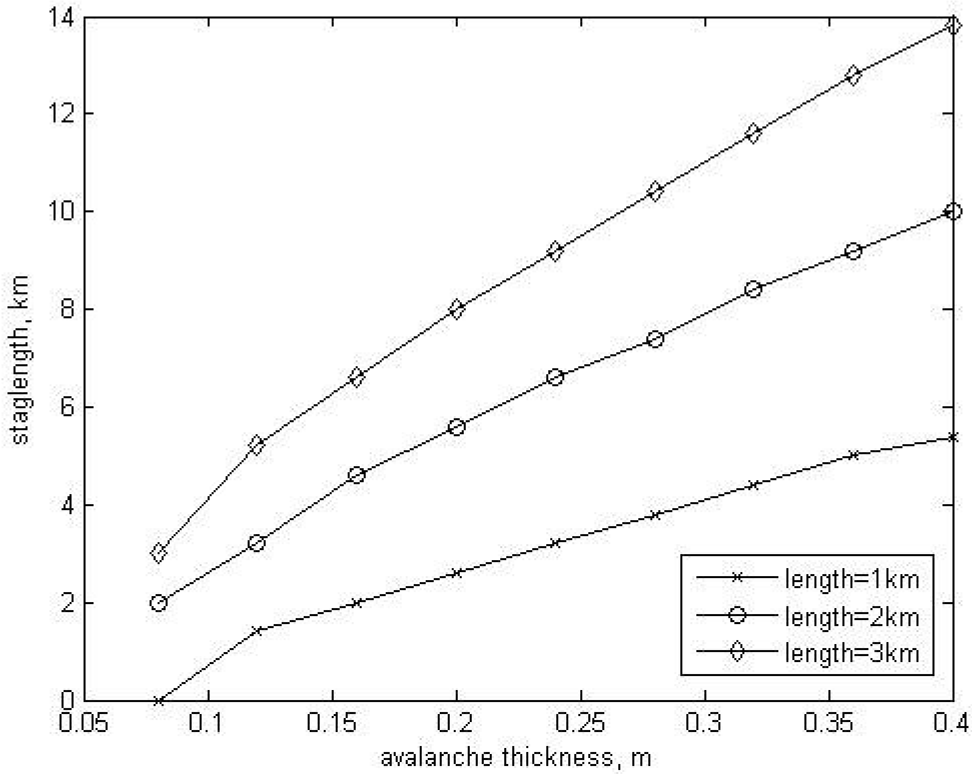

Figure 3.1.6. Stagnation lengths plotted against avalanche layer thickness, m.

Experiments with increasing e-folding thickness for the thermal effect of debris do not greatly affect the results here, beyond the obvious effect that a proportionally thicker debris layer is required to achieve the same effect on the glacier.

In the Waiho Loop experiments, an avalanche of sufficient size to supply the sediment volume in the moraine to the ice front must be ~5 times larger than the Waiho Loop, representing 50 x 10^5 m^2 in the 1D model domain. The runs shown in Figure 3.1.7 required an unphysically large increase of the thermal e-folding thickness from H_r* = 10 cm to H_r* = 50 m (with an e-folding length of H_r* = 10 cm, the glacier advances far into the Tasman Sea, given avalanche volumes much smaller than the Waiho Loop; allowing for spreading at the mouth of the valley would not be sufficient to offset this excessive advance). A 15-km advance is then simulated over ~110 years, producing a layer of sediment ~30 m thick and 15 km long atop stagnant ice, which downwastes over the next ~200 years. An even larger e-folding length could bring the new terminus closer to the actual Waiho Loop, but would leave an even thicker deposit upglacier of the terminus. Given other differences between our model runs and the real glacier, exact tuning was not attempted; the key result is that the modeling shows no physically plausible way for a landslide-triggered advance to avoid thick and laterally extensive deposition in the region crossed by that advance.

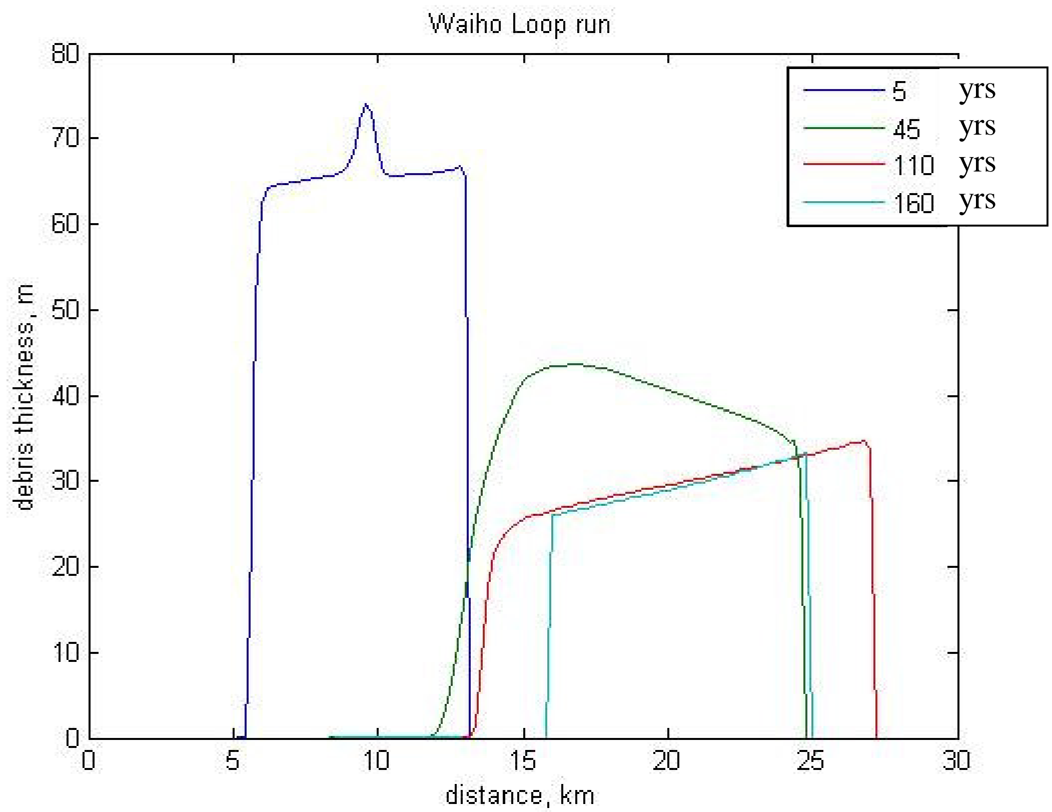

Figure 3.1.7. Snapshots of the supraglacial debris from the Waiho Loop avalanche experiment. After 110 years, glacial advance triggered by avalanche ceases, and 15 km of ice stagnates in the ablation zone.

3.1.6. Discussion

In all of our modeling runs, a rock avalanche causes the glacier to advance, and then stagnate. The ice surface velocities are divergent throughout advance except very near the advancing toe, causing spreading and thinning of the initial avalanche package. Advection of surficial debris eventually causes the location of the initial glacial terminus to become sediment-free. Increased melting at this location causes the section of advancing ice to become malnourished as the mass flux across that location drops to zero. The low flow velocities in the stagnant ice block would cause any supraglacial debris to be deposited in place, as a result of downwasting.

Our experiments indicate that no more than ~20% of a supraglacial debris avalanche reaches a terminal moraine for the advancing debris-covered lobe, so a very large avalanche would be required to generate a Waiho Loop-sized moraine. Such an avalanche would trigger an advance far beyond the Waiho Loop, unless an unphysically large e-folding length for the thermal effects of the debris is specified, and would leave thick and widespread deposits upglacier of the terminal moraine, apparently inconsistent with observations.

Thick debris cover has the potential to greatly reduce mass loss in ablation zones, with important implications for the extent and behavior of glaciers. Additional model experiments (Vacco, 2009, Chapter 3.2) reveal a rich suite of phenomena. However, the modeling also reveals important shortcomings in our understanding of debris effects. We have only sparse direct observations of motion of supraglacial debris on ice, of effective thermal e-folding lengths, and of any dependence of these on glacier character (we suspect that debris redistribution processes are somewhat different on the tongue of the Tasman Glacier than they are on a small cirque glacier, for example).

With existing uncertainties, we do not place much faith in the exact quantitative results of our modeling for application to the natural world. Qualitatively, however, similar glacial responses to avalanches occur in all simulations, and these are sufficiently consistent with our physical understanding that we consider them to be reliable. If a landslide provides sufficient debris cover to reduce melting and trigger a significant glacier advance, the debris remains distributed on the glacier surface and eventually induces stagnation.

3.1.7. References

Agassiz, L.,1845. Les glaciers et le terrain erratique du reversméridional du Mont-Blanc. In: Desor, E. (Ed.), Nouvelles excursions et séjours dans les glaciers et les hautes regions des Alpes de M. Agassiz et de ses compagnons de voyage. Kissling, Neuchâtel.

Anderson, R. S. (2000) A model of ablation-dominated medial moraines and the generation of debris-mantled glacier snouts. *Journal of Glaciology* 46 (154): 459-469.

Conway, H., Gades, A., and Raymond, C. F., 1996, Albedo of dirty snow during conditions of melt. *Water resources research* 32:66, p. 1713-1718.

Conway, H., and Rasmussen, L. A., Summer temperature profiles within supraglacial debris on Khumbu Glacier, Nepal. IN: Nakawo, M., Raymond, C. F., and Fountain, A., *Debris-Covered Glaciers*, IAHS publication no 264, 2000.

D'Agata, C., and Zanutta, A., Reconstruction of the recent changes of a debris-covered glacier (Brenva Glacier, Mont Blanc Massif, Italy) using indirect sources: Methods, results and validation. *Global and Planetary Change* 56 (1-2), p. 57-68.

de Saussure,H.-B.,1786. Voyages dans les Alpes, Précédés d'un Essai sur l'HistoireNaturelle des Environs de Genève. Tome second. Barde, Manguet & Compagnie. Genève

Deline, P., and Kirkbride, M. P., 2009, Rock avalanches on a glacier and morainic complex in Haut Val Ferret (Mont Blanc Massif, Italy). *Geomorphology* 103, p. 80-92.

Denton, G.H., and Hendy, C.H., 1994, Younger Dryas age advance of Franz Josef Glacier in the southern Alps of New Zealand: *Science*, v. 264, p. 1434-1437.

Haidong, H., Yongjing, D., and Shiyin, L., 2006, A simple model to estimate ice ablation under a thick debris layer. *Journal of Glaciology* 52 (179), p. 528-536.

Hanks, T. C., The age of scarplike landforms from diffusion equation analysis. In: J.S. Noller, J.M. Sowers and W.R. Lettis, Editors, *Quaternary Geochronology, Methods and Applications*, American Geophysical Union, Washington, DC (2000), pp. 313–338.

Hansen, J., and Nazarenko, L., 2004, Soot climate forcing via snow and ice albedos, *Proceedings of the National Academy of Sciences*, vol. 101 no. 2 423-428;

Hewitt, K., 2009, Rock avalanches that travel onto glaciers and related developments, Karakoram Himalaya, Asia. *Geomorphology* 103, p. 66-79.

Hochstein, M. P., Claridge, D., Henrys, S. A., Pyne, A., Nobes, D. C., and Leary, S. F., 1995, Downwasting of the Tasman Glacier, South Island, New Zealand: changes in the terminus region between 1971 and 1993. *New Zealand Journal of Geology and Geophysics, Vol. 38*: p. 1-16

Kirkbride, M. P., 1995, Relationships between temperature and ablation on the Tasman Glacier, Mount Cook National-Parl, New Zealand. *New Zealand Journal of Geology and Geophysics* 38, no. 1, p. 17-27.

Kirkbride, M. P., Ice-marginal geomorphology and Holocene expansion of debris-covered Tasman Glacier, New Zealand. IN: Nakawo, M., Raymond, C. F., and Fountain, A., *Debris-Covered Glaciers*, IAHS publication no 264, 2000.

Larsen, S. H., Davies, T. R. H., and McSaveney, M. J., 2005, A possible coseismic landslide origin of late Holocene moraines of the Southern Alps, New Zealand. *New Zealand Journal of Geology & Geophysics* 48, p. 311-314.

Martin, Y., 2000, Modelling hillslope evolution: linear and nonlinear transport relations. Geomorphology 34, no 1-2, p, 1-21.

Mattson, L. E., 2000, The influence of a debris cover on the midsummer discharge of Dome Glacier, Canadian Rocky Mountains. IN: Nakawo, M., Raymond, C. F., and Fountain, A., *Debris-Covered Glaciers*, IAHS publication no 264, 2000.

Pelto, M. S., Mass balance of adjacent debris-covered and clean glacier ice in the North Cascades, Washington. IN: Nakawo, M., Raymond, C. F., and Fountain, A., *Debris-Covered Glaciers*, IAHS publication no 264, 2000.

Schomacker, A., 2008, What controls dead-ice melting under different climate conditions? A discussion. *Earth-Science Reviews* 90, 103-113.

Tovar, D. S., Shulmeister, J., and Davies, T. R., 2008, Evidence for a landslide origin of New Zealand's Wiaho Loop moraine. *Nature Geoscience* 1, p. 524-526.

Vacco, D. A., 2009, Modeling of glacial response to climate changes, including moraine deposition and stagnation events. *Doctoral Dissertation*, Department of Earth and Mineral Sciences, Pennsylvania State University, 101 p.

Van Der Veen, C. J. (1999). *Fundamentals of Glacier Dynamics*. Rotterdam, Balkema.

3.2 Additional Modeling Experiments of Supraglacial Debris on Glaciers.

3.2.1 Introduction

The manuscript of Chapter 3.1 was a study of rock avalanches causing glacier change. In this section, we expand the modeling of supraglacial debris to include a source term from surficial ice melting. We infer that some glaciers containing englacial debris, become covered in supraglacial debris via melt-out. In this study, we test how such "dirty" glaciers respond to climate changes.

3.2.2 Debris source: englacial sediment

We must quantify the melt-out of englacial material as a source for supraglacial debris. Boulton (1970) observed that supraglacial debris is often sourced by the melt out of englacial material. Some debris can be added to the base of a glacier, by processes such as regelation, freeze-on, and stream transport (Alley et al., 1997), and exposed by melting (Lawson, 1979; Spedding, 2000). More importantly for developing widespread supraglacial cover, material is added by mass wasting of valley sides and headwalls, or by debris-bearing basal zones being trapped in englacial positions at the confluences of tributary glaciers to contribute to medial moraines.

Because we are conducting 1-dimensional modeling for this first exploration, the laterally variable debris supply from medial moraines, landslides and other mass-wasting from headwalls is not resolved. Instead, we assume that ice contains a constant, uniform concentration of englacial debris, that is exposed at the surface at a rate proportional to the melting rate. If we set c = concentration of englacial debris, kg/m^3, then the source term from melt-out takes the form:

$$\dot{h}_r = \left(\frac{c}{\rho_{debris}} \right) \dot{m} , \qquad (3.2.1)$$

where ρ_{debris} = the mass density of supraglacial debris in kg/m^3, $\dot{m}$ = the surface melt rate of the ice in m/yr, and $\dot{h}_r$ = the rate of mass delivery to the ice surface, in m/yr.

3.2.3 Supraglacial debris equation in one-dimension

The governing equation used for these modeling experiments takes the form:

$$\frac{dh_r}{dt} = -u_i(s_i)\frac{\partial h_r}{\partial x} + k\frac{\partial^2 s_r}{\partial x^2} + \left(\frac{c}{\rho_{debris}} \right) \dot{m} , \qquad (3.2.2)$$

where h_r = supraglacial debris thickness, s_i = ice surface elevation, u_i = ice flow velocity in m/yr, k = diffusivity of debris in m^2/yr, and s_r = supraglacial debris surface elevation. Debris can be transported by advection along the ice surface or by down-slope diffusion (mass wasting), and mass enters the system by ice surface melting. The glacier limits represent infinite mass sinks, through which debris cannot re-enter the system. (In subsequent work, deposition of this material can be allowed, following Vacco et al. (in press (a)).

3.2.4 Experiment description, englacial debris source

The one-dimensional experiments were run on a planar sloping bed (at 4% slope). The ice model was run under constant climate until it reached steady state, allowing melting to supply debris to the ice surface. Upon reaching steady state, an instantaneous warming was applied to the system, ranging from 0.5 – 1.0 ^{o}C, and the model was run until a new steady state was established.

The experiments were run for englacial debris concentrations ranging from c = 0 kg/m^3 to 4.5 kg/m^3, incremented by 0.5 kg/m^3, representing 0 – 0.2 % sediment by volume. The diffusivity of debris was the same across all runs, k = 0.1 m^2/yr. Stagnation events were recorded if, during the warming phase of the experiment, the ice flow velocity decreased to less than 0.1 m/yr, and the ice thickness was greater than 10.0 m. During the warming phase of the model runs, the location of stagnant ice was recorded, and any readvance of the active ice terminus was assumed to “erase” underlying stagnation deposits.

3.2.5 Experiment results and discussion, englacial sediment source

Warming caused retreat without stagnation in the clean-ice case, but stagnation in all debris-bearing cases (figure 3.2.1 through figure 3.2.8). In the cases containing englacial debris, during the retreat, the velocities drop below 2 cm/yr in sections of non-zero ice thickness (Figure 3.2.3 and Figure 3.2.4, 20 years after warming, and Figure 3.2.6 and Figure 3.2.7, 30 years and 60 years after warming). The glaciers containing debris undergo readvance after retreat (Figure 3.2.3, Figure 3.2.6). Increased englacial debris corresponds to longer steady state ice profiles, pre-warming, (Figure 3.2.9) and more supraglacial debris (Figure 3.2.10).

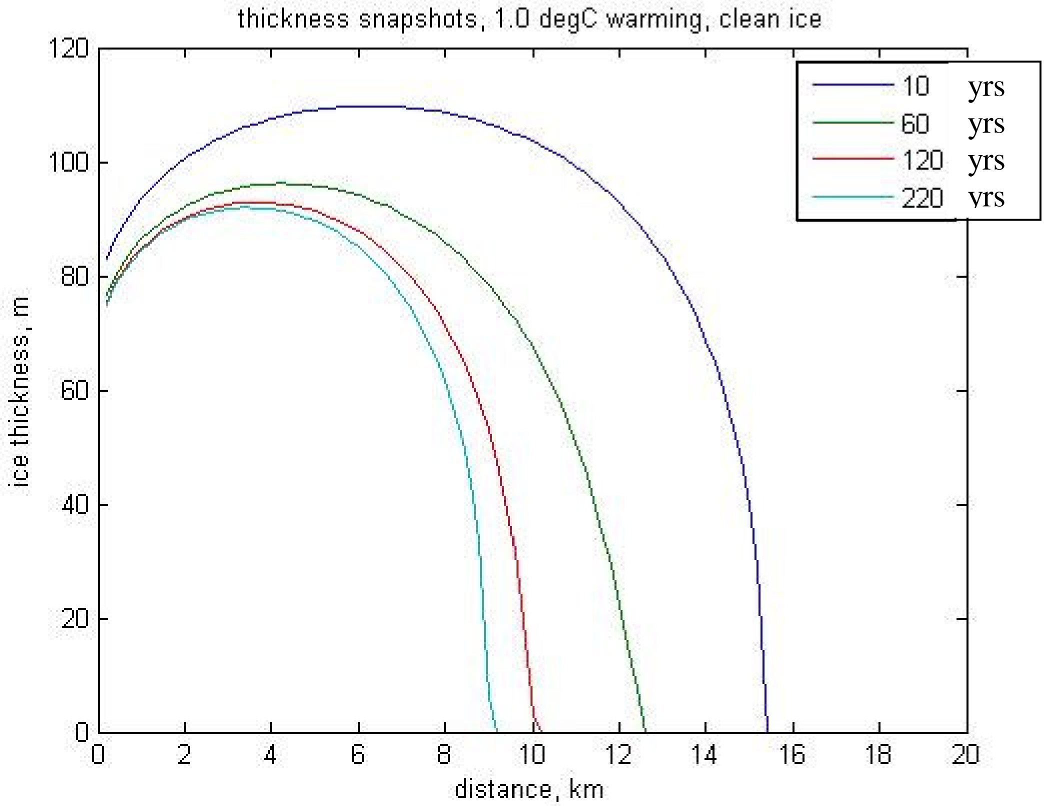

Figure 3.2.1. Ice thickness snapshots after 1.0 ^{o}C warming, for clean ice. The bed is a planar sloping surface at 4% slope.

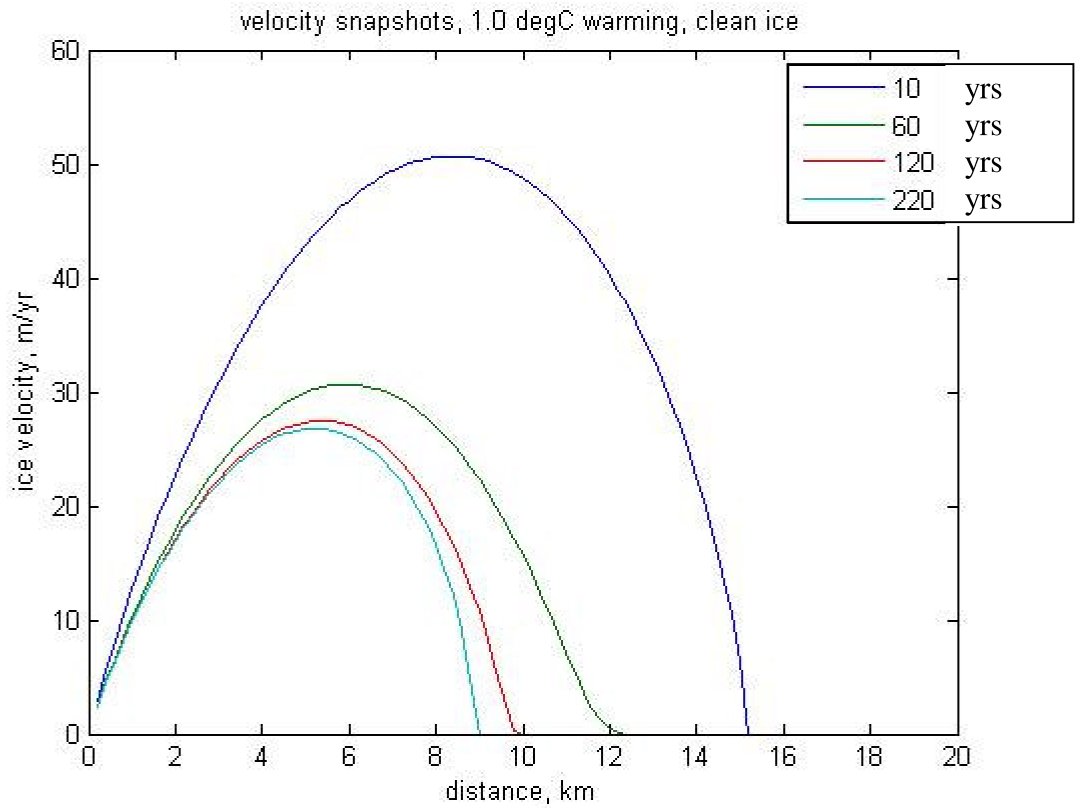

Figure 3.2.2. Ice velocity snap shots after 1.0 ^{o}C warming, for clean ice.

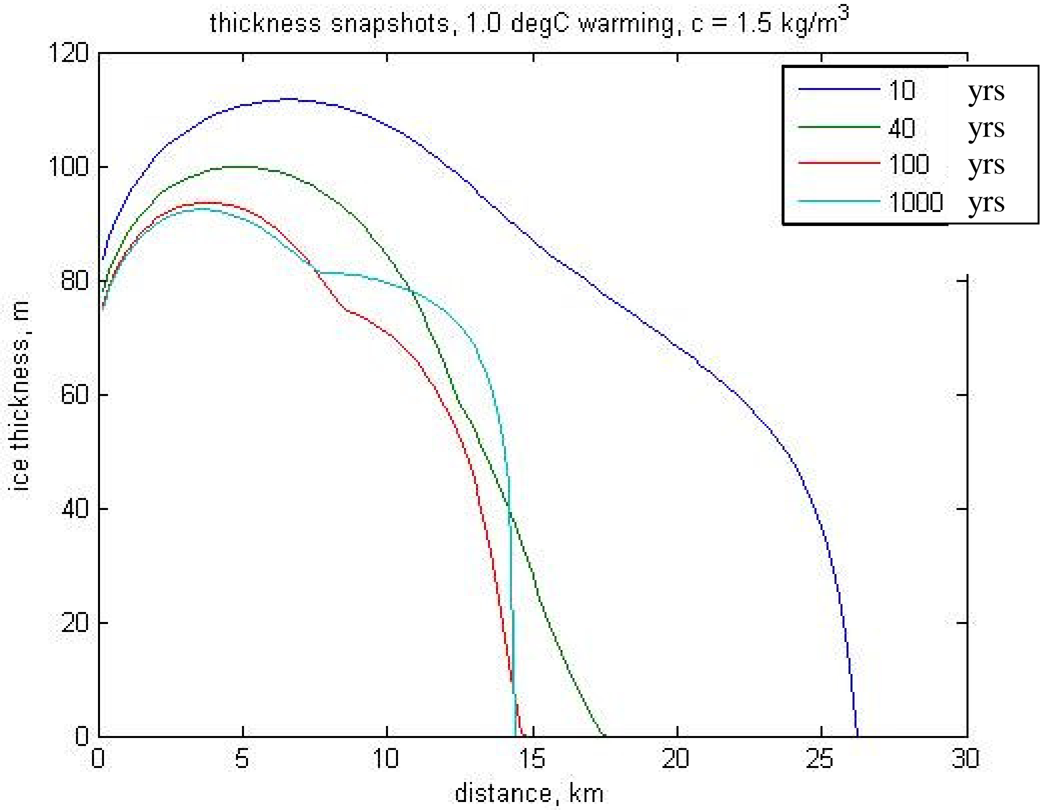

Figure 3.2.3. Ice thickness snapshots after 1.0 °C warming, for ice with englacial debris concentration C = 1.5 kg/m^3.

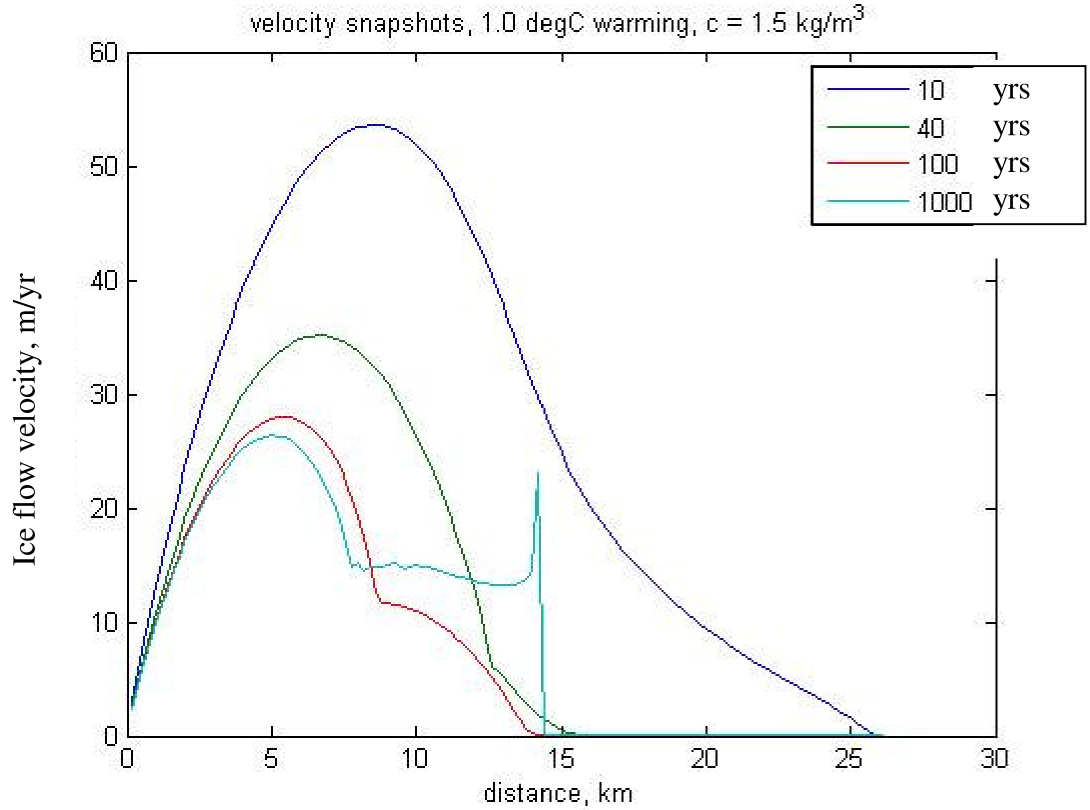

Figure 3.2.4. Ice velocity snapshots after 1.0 ^{o}C warming, for debris concentration c = 1.5 kg/m^3.

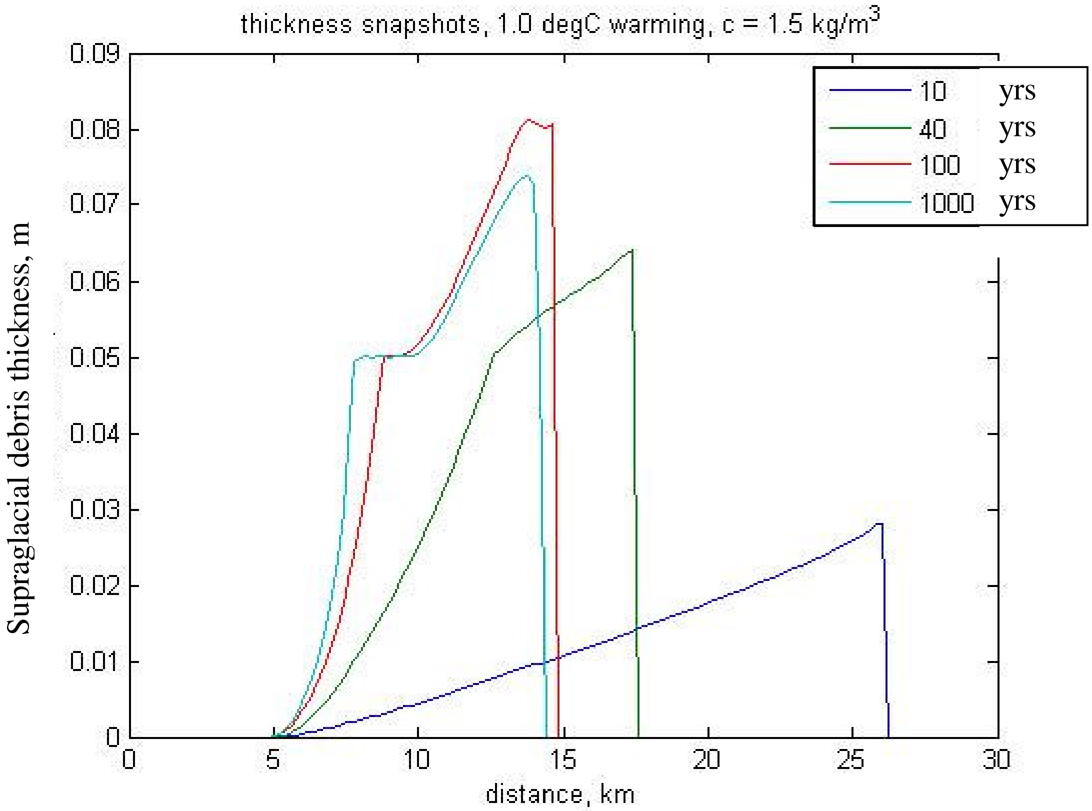

Figure 3.2.5. Supraglacial debris snap shots after 1.0 ^{o}C warming, for englacial debris concentration c = 1.5 kg/m^3.

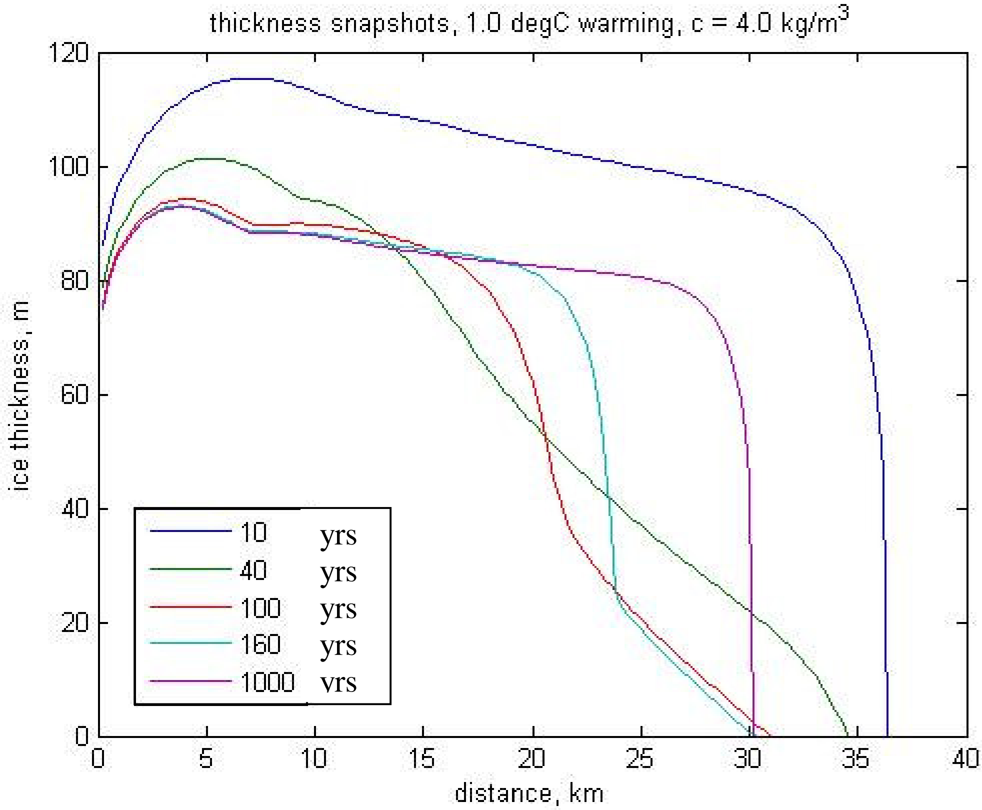

Figure 3.2.6. Ice thickness snap shots after 1.0 ^{o}C warming, for englacial debris concentration c = 4.0 kg/m^3.

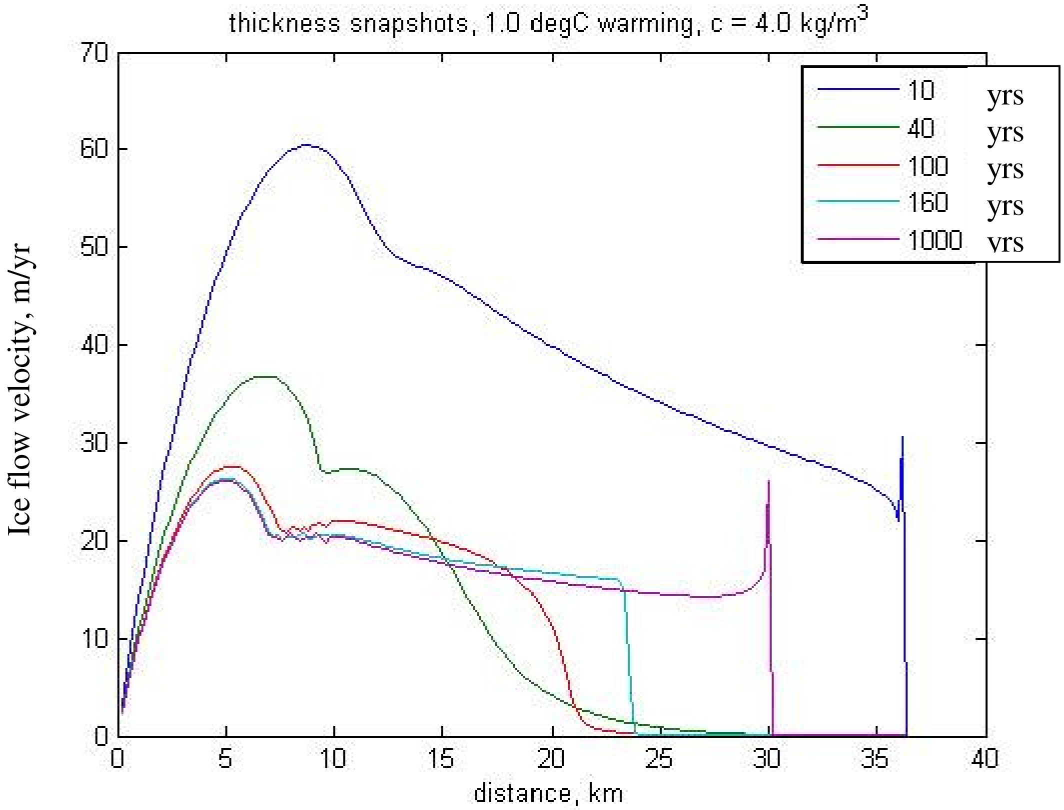

Figure 3.2.7. Ice flow velocity snap shots after 1.0 ^{o}C warming, englacial debris concentration c = 4.0 kg/m^3.

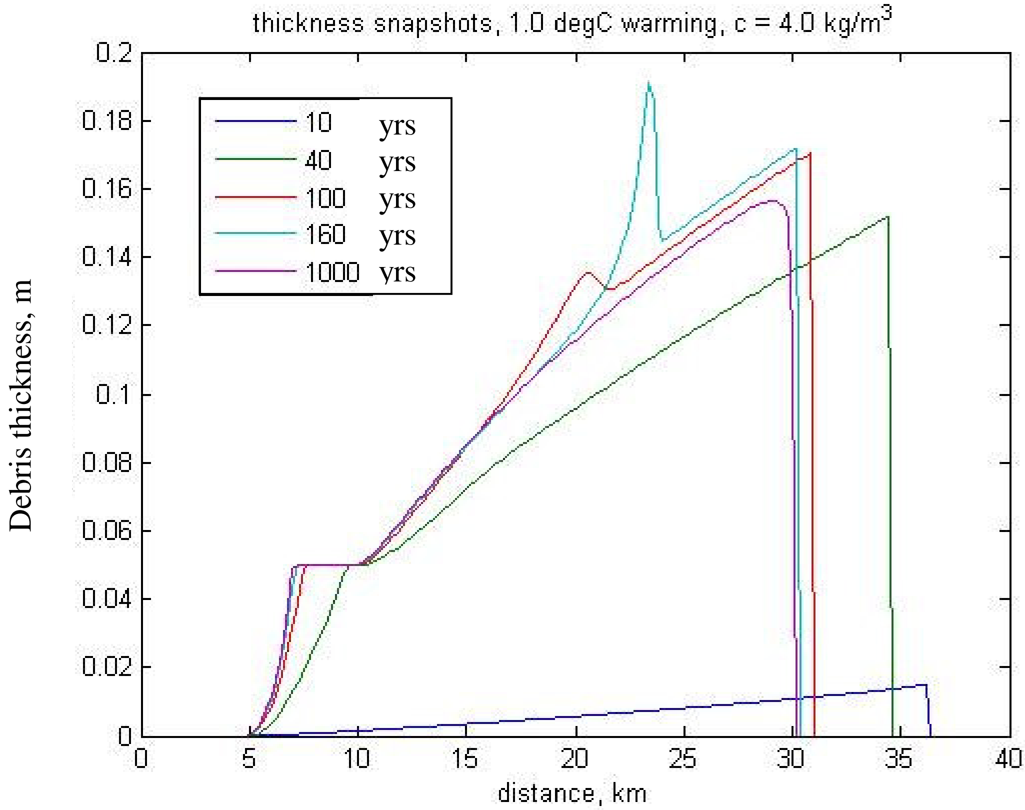

Figure 3.2.8. supraglacial debris thickness snapshots after 1.0 ^{o}C warming, englacial debris concentration c = 4.0 kg/m^3.

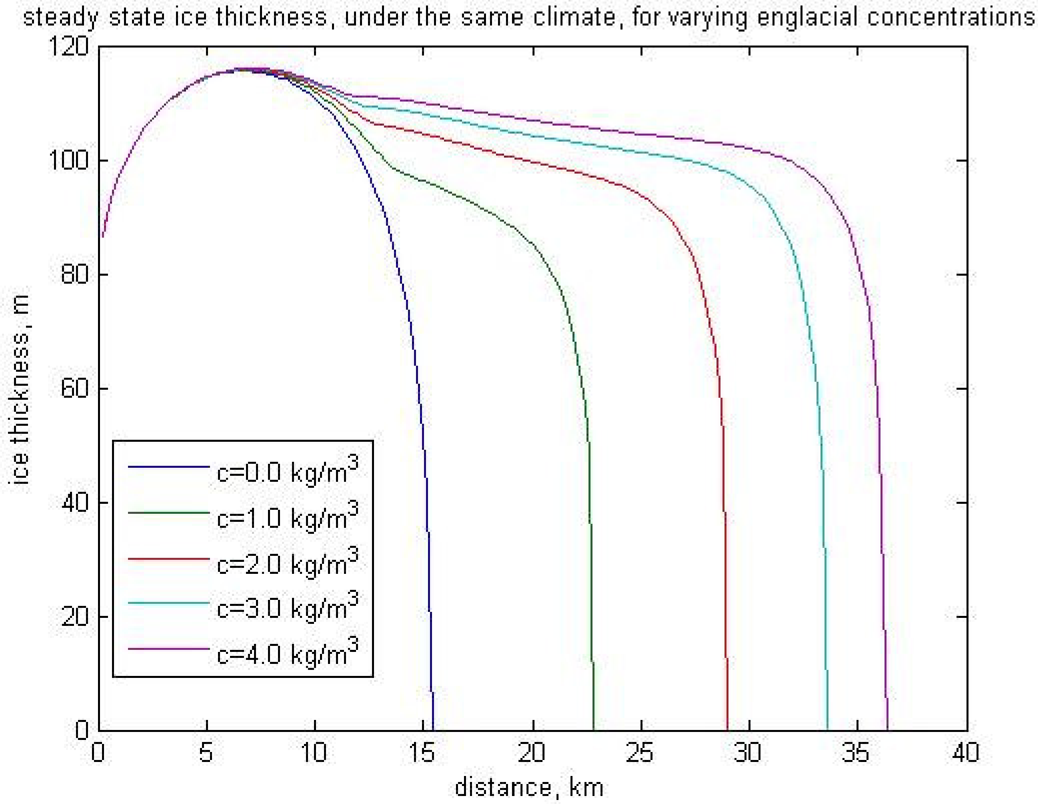

Figure 3.2.9. Steady state ice thickness distribition, under uniform climate, for different values of englacial concentration.

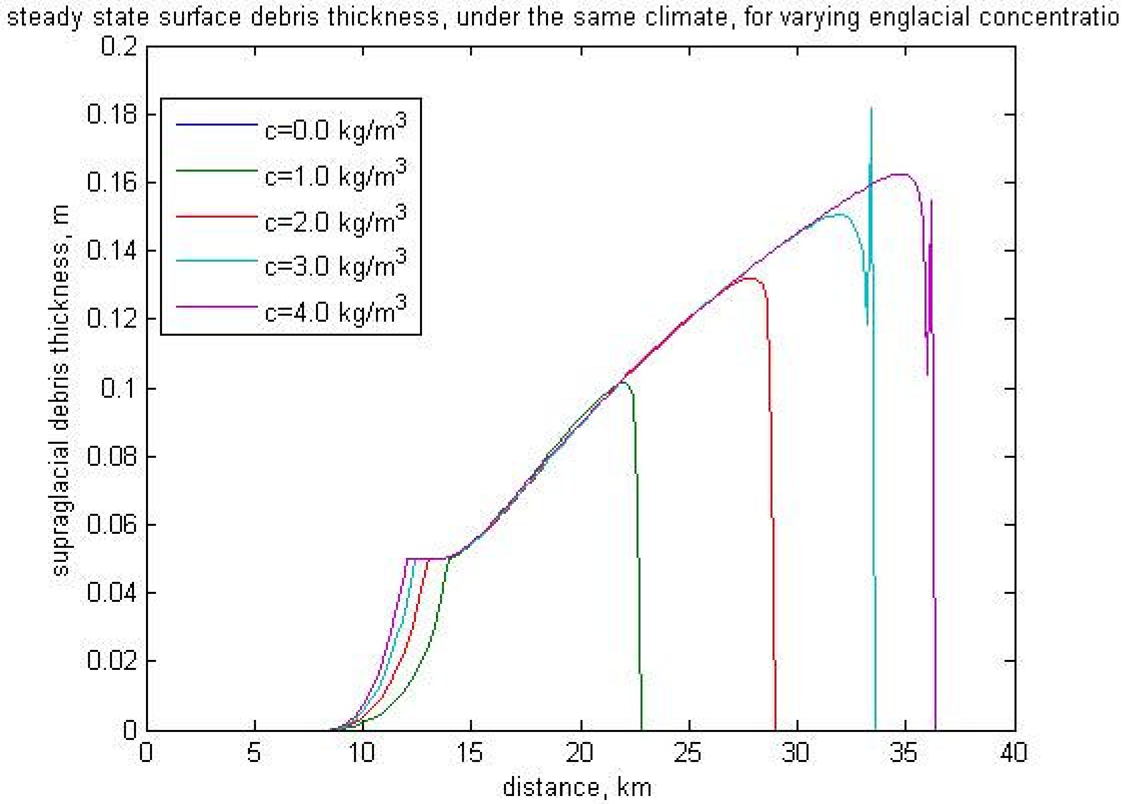

Figure 3.2.10. supraglacial debris distributions on steady state glacier, given uniform climate conditions, for varying values of englacial debris concentration.

As the concentration of englacial debris was increased from zero, the total length of stagnation increased (Figure 3.2.11). However, above a concentration of 2.0 kg/m^3, the stagnation length decreased with increasing concentration of debris. At these very high debris concentrations, warming causes the terminal region to stagnate, but the region upglacier that shifts from accumulation to ablation becomes sufficiently debris-covered to trigger an advance that partially overruns the region of initial stagnation, and this secondary advance increases with increasing debris load. In these high-debris warming experiments, the new steady-state glacier is shorter than the original glacier, but the active toe experiences a large retreat followed by a smaller readvance.

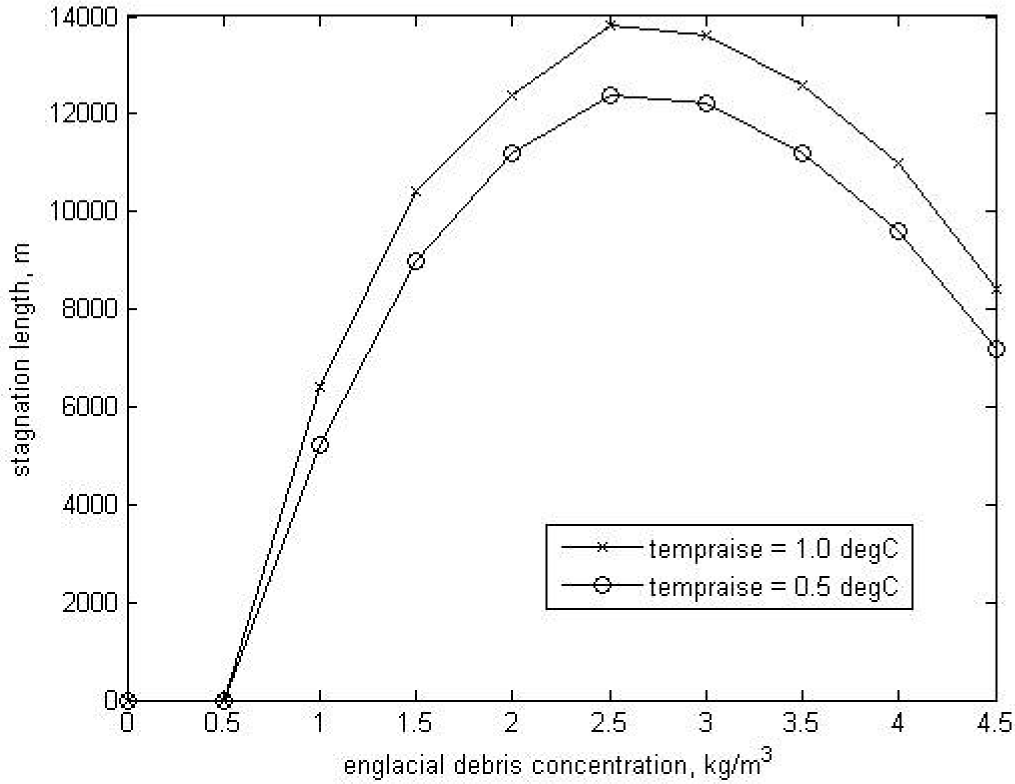

Figure 3.2.11. Stagnation lengths against englacial debris concentration. Plotted are results under 0.5 °C instant warming (-o-) and 1.0 °C warming (-x-). Stagnation length increases up to 2.5 kg/m3, but decreases with higher concentration because increasing debris leads to increased shielding.

3.2.6 Discussion of results

In every case, including the melt-out of englacial sediment led to a stagnation event, with concentrations > 0.5 kg/m^2. The control experiment, a debris-free glacier, did not stagnate under the same conditions. These experiments were run for a planar sloping bed, a setting in which clean ice does not stagnate under any magnitude of warming. The concentrations of englacial debris that were tested were relatively low (<0.2 % by volume), considering the multiple sources for entrainment of englacial sediment (Alley et al., 1997).

These experiments confirm the strong role that supraglacial sediment plays in the onset and magnitude of glacial stagnation. Non-climatic factors, including rock avalanches, and other sources of glacial sediment, clearly have an effect on the character of glacial response to climate changes. This study indicates that the size of an observed stagnation field is not necessarily a direct result of the warming that forced glacial change, that the amount of sediment on the ice surface is also significant.
Vacco et al. (in press b) showed how to account for the effects of topography and climatic change on the tendency for stagnation, and the current study adds debris cover.

Given appropriate knowledge of debris supply, warming magnitude and rate, glacier-bed topography and basal lubrication, it is possible to conduct forward models of glacial stagnation. Probably the largest uncertainty in this forward modeling is related to the effective e-folding length for the thermal effects of supraglacial debris. As discussed in 3.1, observations including those on Tasman Glacier show that local redistribution of sediment on the surface of a debris-bearing glacier reduces without eliminating the thermal effect of that debris; however, this remains poorly quantified.

A key goal of these studies is to enable inverse modeling, allowing the presence or absence of stagnation deposits of given age in various glacial valleys of a region to be used to learn the size or rate of warming responsible for the retreat/stagnation behavior (chapter 2). Information on the sediment loading may be available from the volume of stagnation deposits, or might be parameterized from observed characteristics of basins (length of headwalls, etc.). With appropriate data on melt rates of debris-covered glacier toes, and thus on the effective thermal effect of debris cover, this inverse modeling may be possible.

3.2.6 References

Alley, R. B., K. M. Cuffey, E. B. Evenson, J. C. Strasser, D. E. Lawson and G. J. Larson,1997, How Glaciers Entrain and Transport Basal Sediment: Physical Constraints. *Quaternary Science Reviews* 16, 1017-1038 .

Anderson*,* R. S. 2000, A model of ablation-dominated medial moraines and the generation of debris-mantled glacier snouts. *Journal of Glaciology* 46 (154): 459-469.

Boulton, G. S., 1970, On the origin and transport of englacial debris in Svalbard glaciers, *Journal of Glaciology* **9**, pp. 213–229.

Hanks, T. C., The age of scarplike landforms from diffusion equation analysis. In: J.S. Noller, J.M. Sowers and W.R. Lettis, Editors, *Quaternary Geochronology, Methods and Applications*, American Geophysical Union, Washington, DC (2000), pp. 313–338.

Lawson, D.E., Sedimentological analysis of the western terminus region of the Matanuska Glacier, Alaska. *CRREL Report 79-9* (1979).

Martin, Y., 2000, Modelling hillslope evolution: linear and nonlinear transport relations. *Geomorphology* 34, no 1-2, p, 1-21.

Spedding, N., Hrodrological controls on sediment transport pathways: implications for debris-covered glaciers. IN: Nakawo, M., Raymond, C. F., and Fountain, A., *Debris-Covered Glaciers*, IAHS publication no 264, 2000.

Vacco, D. A., Alley, R. B., and Pollard, D., in press (a), Modeling dependence of moraine deposition on climate history: the effect of seasonality. Quaternary Science Reviews (2008), doi:10.1016/j.quascirev.2008.04.018

Vacco, D. A., Alley, R. B., and Pollard, D., in press (b), accepted, Numerical Modeling of Valley Glacier Stagnation: Toward a new Paleoclimatic Indicator. *Quaternary Research* (2009).

3.3 Conclusions, and Future Work

The modeling results of Chapter 3 indicate that supraglacial debris has a strong role in the stagnation of glaciers. The results of chapter 2 indicate that bumpy beds play a role in stagnation events, but it has become clear that supraglacial debris can cause stagnation events in almost any glacial setting. Much work remains to be done to improve the supraglacial debris model to a point where it can be used to make quantitative predictions of natural stagnation events.

Most importantly, we need to collect observations of the elevations and geologic settings of debris covered glaciers, for the purpose of constraining the mechanisms and rates of delivery of sediment to the glacier surface. Rock avalanche rates are a function of valley wall topography, glacial erosion rates, climate factors, and lithology. It is possible that these characteristics can be parameterized such that a deterministic relationship can be derived between glacial valley geology and avalanche rates.

Additionally, we must consider the presence and amounts of englacial debris in glaciers. Many glaciers are "clean," containing very little debris. Our modeling results, however, indicate that very small amounts of englacial debris (0.02 % by volume) can lead to delivery of significant amounts of debris to the glacial surface. Modeling the sources and rates of delivery of englacial debris to the glacier body is relatively unconstrained, and it is important to quantify these for our forward modeling purposes.

The ice flow modeling of this study applied the shallow ice approximation for glacier flow. It is well documented that the shallow ice approximation poorly represents the glacier toe. In the modeling of supraglacial debris, the glacial toe behavior has a very significant effect on the development of debris, including its advection, distribution, and final deposition. In order to more accurately model the dynamics of supraglacial debris, we must improve our ice flow modeling to include longitudinal stresses. This will aid our purpose of modeling glacial terminus behavior more accurately.

In addition to further exploration of the supraglacial debris model itself, there also remains much to be explored with glacial response to supraglacial debris. There are many, as yet unexplored, feedbacks between glacier changes and supraglacial debris changes. Our modeling in this study involved steady state glacier criteria, but rarely to glaciers in nature reach a steady state. Possible stagnation events within a changing climate, including feedback effects of changing climate on sediment delivery to the glacier surface, are likely to have played a role in many observed stagnation events.

The ultimate question regarding supraglacial debris and stagnation is if we can recover climate change from observed stagnation deposits. The work of chapter 2 indicated that we could directly infer climate change magnitude from measurements of stagnation deposits. The discoveries of chapter 3, specifically that avalanches can trigger stagnation events, show us that the cause-and-effect relationship between climate change and stagnation is not explicit.

DAVID A. VACCO
Penn State Ice and Climate Exploration (PSICE)
Department of Geosciences
532 Deike Bldg., Pennsylvania State University, University Park, PA, 16802
Email: dvacco@geosc.psu.edu, phone: 585-738-9374

Degrees

Monroe Community College, Liberal Arts,	1998; A.S.
SUNY Geneseo, Geological Sciences major, Mathematics minor,	2001; B.A.
Oregon State University, Geology,	2003; M.S.
Pennsylvania State University, Geology,	2009; Ph.D.

Publications

Vacco, D. A., Alley, R. B., and Pollard, D., in review 2008, Numerical Modeling of Valley Glacier Stagnation: Toward a New Paleoclimatic Indicator. *Quaternary Research*, Elsevier.

Vacco, D. A., Alley, R. B., and Pollard, D., in press 2008, Modeling the evolution of deglaciation moraines. *Quaternary Science Reviews*, special issue, Tribute to Geoffrey S. Boulton.

Vacco, D.A., Clark, P.U., Mix, A.C., Cheng, H., and Edwards, R.L., 2005, A speleothem record of Younger Dryas cooling from the Klamath Mountains, Oregon: *Quaternary Research*, v. 64, p. 249-256.

Vacco, D. A., Developing climate records from speleothems, Oregon Caves National Monument. *Master's thesis*, Oregon State University (2003).

Vacco, D. A., Geochemistry of a modern anoxic environment, Buck Run, Mount Morris, Livingston County, New York. SUNY *Geneseo Journal of Science and Mathematics*, **2**(1), 35-42, (2001).

Collaborators and other affiliations

1. Collaborators: R. B. Alley (PSU), Applegate, P. (PSU), H. Cheng (UMinn), P. U. Clark (OSU), T. K. Dupont (PSU), R. L. Edwards (UMinn), A. C. Mix (OSU), B. R. Parizek (PSU), D. Pollard (PSU), R. A. Young (Geneseo).

Graduate Advisors: R. B. Alley (Ph.D., Penn State), P. U. Clark (M.Sc., Oregon State).